Nickel-pincer cofactor biosynthesis involves LarB-catalyzed pyridinium carboxylation and LarE-dependent sacrificial sulfur insertion

Benoît Desguin[a,b], Patrice Soumillion[b], Pascal Hols[b], and Robert P. Hausinger[a,1]

[a]Department of Microbiology and Molecular Genetics, Michigan State University, East Lansing, MI 48824; and [b]Institute of Life Sciences, Université catholique de Louvain, B-1348 Louvain-La-Neuve, Belgium

Edited by Tadhg P. Begley, Texas A&M University, College Station, TX, and accepted by the Editorial Board March 28, 2016 (received for review January 11, 2016)

The lactate racemase enzyme (LarA) of *Lactobacillus plantarum* harbors a (SCS)Ni(II) pincer complex derived from nicotinic acid. Synthesis of the enzyme-bound cofactor requires LarB, LarC, and LarE, which are widely distributed in microorganisms. The functions of the accessory proteins are unknown, but the LarB C terminus resembles aminoimidazole ribonucleotide carboxylase/mutase, LarC binds Ni and could act in Ni delivery or storage, and LarE is a putative ATP-using enzyme of the pyrophosphatase-loop superfamily. Here, we show that LarB carboxylates the pyridinium ring of nicotinic acid adenine dinucleotide (NaAD) and cleaves the phosphoanhydride bond to release AMP. The resulting biscarboxylic acid intermediate is transformed into a bisthiocarboxylic acid species by two single-turnover reactions in which sacrificial desulfurization of LarE converts its conserved Cys176 into dehydroalanine. Our results identify a previously unidentified metabolic pathway from NaAD using unprecedented carboxylase and sulfur transferase reactions to form the organic component of the (SCS)Ni(II) pincer cofactor of LarA. In species where *larA* is absent, this pathway could be used to generate a pincer complex in other enzymes.

lactate | racemase | nicotinic acid dinucleotide | sacrificial enzyme

Lactate racemase (Lar) interconverts D- and L-lactic acid, providing microorganisms with the ability to use or produce both isomers even if only one stereospecific lactate dehydrogenase is present. The enzyme (LarA) harbors a covalently bound Ni pyridinium-3-thioamide-5-thiocarboxylic acid mononucleotide pincer complex featuring a Ni–C bond (Fig. 1*A*) (1). A pincer ligand in organometallic chemistry traditionally consists of a central ring disubstituted with two chelating side arms (2). The central atom together with the two donor groups on the side arms bind to the metal ion in a planar fashion, providing both structural and thermal stability (2). Many nickel pincer complexes have been synthesized to stabilize the nickel ion and control its reactivity, some of them exhibiting high catalytic activity (2). Although pincer complexes are ubiquitous in synthetic chemistry, the LarA cofactor is the first example of a pincer compound identified in the natural world. This cofactor, thought to reversibly capture hydride from the substrate, is synthesized from nicotinic acid by a pathway requiring LarB, LarC, and LarE. LarE is able to activate the LarA apoprotein when isolated from cells also producing LarB and LarC (3). This result implies that LarE harbors the Ni-containing cofactor before its transfer to LarA. In this study, we describe the biosynthetic pathway leading to the formation of the lactate racemase (SCS)Ni(II) pincer complex starting from the NAD precursor, nicotinic acid adenine dinucleotide (NaAD).

Results

In Vitro LarA Activation. We reconstituted LarA cofactor biosynthesis in vitro by incubating extracts of LarB-containing cells with purified LarC and LarE, along with various additives (*SI Appendix*, Fig. S1*A*). Lar activity was observed for lysates of cells expressing *larB* (used directly or after filtration to remove proteins) when incubated with ATP (1 mM), $MgCl_2$ (12 mM), and the other purified proteins, and the activity was stimulated fivefold by inclusion of CoA (10 mM) (*SI Appendix*, Fig. S1 *A*–*D*). These results are consistent with the requirement of a small molecule produced by LarB being needed for development of Lar activity. To uncover the substrate of LarB, we replaced the LarB-containing lysates in the LarA activation mixture with purified LarB and potential substrates. Because nicotinic acid is a precursor of the Lar cofactor (1) and LarB features partial sequence identity with PurE, an aminoimidazole ribonucleotide (AIR) mutase/carboxylase (4), we tested the possibility that LarB could carboxylate intermediates of the Preiss–Handler pathway from nicotinic acid to NAD (5), namely nicotinic acid mononucleotide (NaMN) and NaAD. Whereas we detected only very low levels of Lar activity when using NaMN, substantial LarA activation was observed for samples incubated with NaAD, and the activity increased with added bicarbonate and Ni^{2+} (Fig. 1*B*). When the LarB reaction was performed separately from the LarC and LarE reactions, significant Lar activity was only observed when LarB was incubated with NaAD and bicarbonate (Fig. 1*C*). ATP and Ni^{2+} were not required for the LarB reaction (Fig. 1*C*).

Pyridinium Carboxylation by LarB. To identify the products of LarB, we performed the in vitro LarB reaction with NaAD, $MgCl_2$, and $NaHCO_3$ or $NaH^{13}CO_3$ and compared the samples by liquid chromatography–electrospray ionization–mass spectrometry (LC-ESI-MS). In the absence of LarB, only NaAD was observed, whereas in the presence of LarB we observed the products of

Significance

Nicotinic acid is a precursor of the ubiquitous cofactors nicotinamide adenine dinucleotide (NAD) and nicotinamide adenine dinucleotide phosphate (NADP). Previous studies revealed that nicotinic acid is required for lactate racemization, an enzymatic activity that enables microorganisms to produce or use both isomers of lactate. Lactate racemase (Lar) was shown to harbor a nicotinic acid-derived cofactor that coordinates a nickel ion, forming a pincer complex. The biosynthesis of this cofactor requires three accessory proteins: LarB, LarC, and LarE. Here, we describe this biosynthetic pathway by showing that LarB carboxylates and hydrolyzes the NAD precursor nicotinic acid adenine dinucleotide (NaAD) and LarE sacrificially inserts two sulfur atoms into the product of LarB. Finally, LarC inserts the nickel ion to form the mature cofactor.

Author contributions: B.D., P.S., P.H., and R.P.H. designed research; B.D. performed research; B.D., P.S., P.H., and R.P.H. analyzed data; and B.D., P.S., P.H., and R.P.H. wrote the paper.

The authors declare no conflict of interest.

This article is a PNAS Direct Submission. T.P.B. is a guest editor invited by the Editorial Board.

[1]To whom correspondence should be addressed. Email: hausinge@msu.edu.

This article contains supporting information online at www.pnas.org/lookup/suppl/doi:10.1073/pnas.1600486113/-/DCSupplemental.

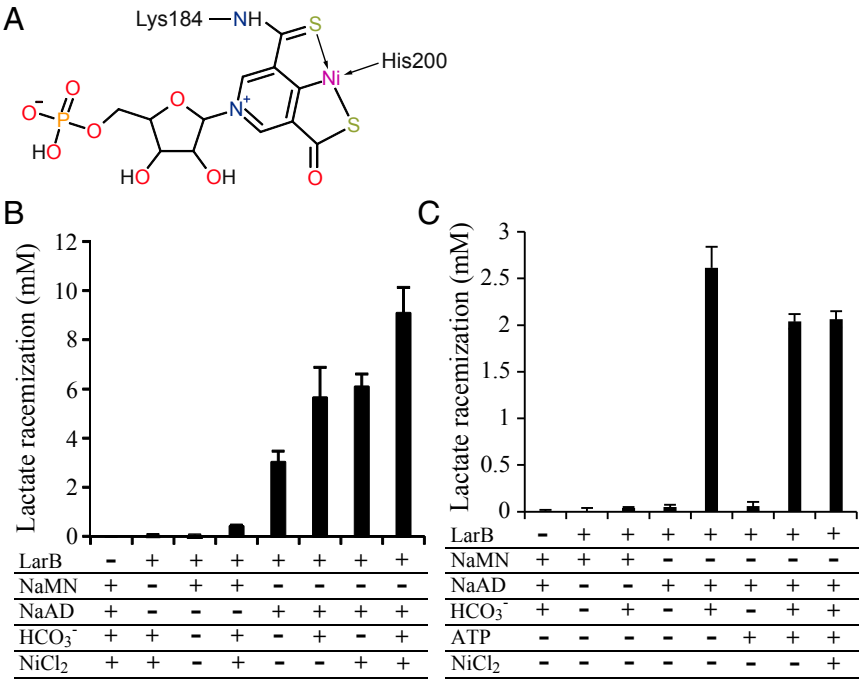

Fig. 1. Identification of the substrate of LarB. (*A*) Structure of the (SCS)Ni(II) pincer cofactor covalently bound to *L. plantarum* LarA and synthesized by LarB, LarC, and LarE. (*B*) Lar activity generated upon addition of LarA apoprotein to solutions incubated for 2 h with LarE (5 μM), LarC (5 μM), $MgCl_2$ (20 mM), ATP (5 mM), and CoA (1 mM) in Tris·HCl buffer (100 mM; pH 8) along with (where indicated) LarB (1 μM), NaMN (0.5 mM), NaAD (0.5 mM), $NaHCO_3$ (10 mM), and $NiCl_2$ (0.1 mM). (*C*) LarB reaction was performed for 10 min in Tris·HCl buffer (100 mM; pH 8) with $MgCl_2$ (4 mM) along with (where indicated) LarB (0.5 μM), NaMN (0.2 mM), NaAD (0.2 mM), $NaHCO_3$ (100 mM), ATP (5 mM), and $NiCl_2$ (0.1 mM) before inactivation and incubation for 1 h with LarE, LarC, $MgCl_2$, ATP, and CoA and addition of LarA apoprotein as in *B*. Error bars represent the SD ($n = 4$).

NaAD hydrolysis, NaMN and AMP (Fig. 2*A*). When we added $NaHCO_3$ to the LarB reaction, however, a species of $m/z = 380.04$ appeared, with this species shifting to $m/z = 381.04$ using $NaH^{13}CO_3$ (Fig. 2*B*). Only the LC fractions containing these species were capable of LarA in vitro activation in the presence of LarC and LarE (*SI Appendix*, Fig. S2). These species correspond to the mass of NaMN plus a carboxyl group ($C_{12}H_{15}NO_{11}P^+$: m/z = 380.038; $C_{11}{}^{13}CH_{15}NO_{11}P^+$: m/z = 381.045). Fragmentation of these ions yielded products consistent with NaMN being carboxylated on the pyridinium ring (*SI Appendix*, Fig. S3). In particular, the unlabeled and isotopically labeled suspected pyridinium-3,5-biscarboxylic acid mononucleotide (P2CMN) species gave rise to $m/z = 168$ and 169 positive ion fragments as expected for the corresponding pyridine biscarboxylates (*SI Appendix*, Fig. S3*A*). The dicarboxylated pyridinium ring formed with ^{13}C can fragment to form NaMN by loss of either the original carboxylate or the ^{13}C carboxylate. Equivalence of these two species (*SI Appendix*, Fig. S3*B*) is consistent with a symmetric structure, thus indicating the site of carboxylation and confirming that LarB is a NaAD carboxylase-hydrolase–forming P2CMN.

We characterized several properties of LarB-catalyzed P2CMN formation by monitoring the in vitro activation of LarA (*SI Appendix*, Fig. S4). We showed that the K_m for NaAD was 13 ± 3 μM (*SI Appendix*, Fig. S4*A*), the K_m for $MgCl_2$ was 0.55 ± 0.18 mM (*SI Appendix*, Fig. S4*B*), and the apparent K_m of $NaHCO_3$ was 33 ± 18 mM (*SI Appendix*, Fig. S4*C*), which are comparable to the values for AIR carboxylation by PurE (6). We found quite different parameters when examining LarB-catalyzed NaAD turnover by assessing AMP release (*SI Appendix*, Fig. S5). The rate of product release appeared to exhibit hyperbolic behavior (with a K_m of 26 ± 15 μM) superimposed on a reaction rate that was linearly dependent on NaAD concentrations (*SI Appendix*, Fig. S5*A*). The K_m for $MgCl_2$ was 3.9 ± 2.2 mM (*SI Appendix*, Fig. S5*B*), whereas AMP release was independent of $NaHCO_3$ concentration (*SI Appendix*, Fig. S5*C*). These results suggest that LarB can hydrolyze NaAD directly or it first forms an adduct with NaAD that releases AMP and reacts with CO_2 to generate P2CMN (*SI Appendix*, Fig. S5*D*).

Sulfur Insertion by LarE. Because the LarA cofactor contains two sulfur atoms (1) (Fig. 1*A*), the role of LarE could be to modify the two carboxylic acids of P2CMN by forming two thiocarboxylic acids. To test this hypothesis, we incubated LarE with P2CMN or ^{13}C-labeled P2CMN (P2CMN*) obtained through the in vitro reaction of LarB with NaAD and $NaHCO_3$ or $NaH^{13}CO_3$, respectively. After incubation, LarE was digested with trypsin, and the solution was analyzed by LC-ESI-MS. We detected species of $m/z = 396.02$ and $m/z = 411.99$ when using P2CMN and of m/z = 397.02 and $m/z = 413.00$ when using P2CMN* (Fig. 2*C*). The molecular masses of these species are consistent with pyridinium-3-carboxy-5-thiocarboxylic acid mononucleotide (PCTMN) and pyridinium-3,5-bisthiocarboxylic acid mononucleotide (P2TMN) ($C_{12}H_{15}NO_{10}SP^+$: $m/z = 396.015$ and $C_{12}H_{15}NO_9S_2P^+$: m/z = 411.993). The two putative PCTMN species (unlabeled and labeled, respectively) gave rise to tandem MS (MS/MS) species (m/z = 184 and 185) that were expected for the corresponding pyridine-3-carboxylate-5-thiocarboxylate fragments (*SI Appendix*, Fig. S6). The two putative P2TMN species (unlabeled and labeled, respectively) similarly gave rise to MS/MS species (m/z = 200 and 201) that were expected for the corresponding pyridine bisthiocarboxylate fragments (*SI Appendix*, Fig. S7). The presence of m/z = 183 and 184 species in the positive-ionization mode and of m/z = 333, 334, 393, and 394 species in the negative ionization mode indicates the presence of pyridinium-3-carboxamide-5-thiocarboxylic acid mononucleotide (*SI Appendix*, Fig. S6), which probably arose as a product of the nucleophilic attack of P2TMN by the ammonia present in solution.

Furthermore, the putative PCTMN and P2TMN species led to m/z = 334 and 350 negative ion fragments, respectively, arising from loss of COS, which is consistent with sulfur insertion into the carboxylic acid groups of P2CMN (*SI Appendix*, Figs. S6 and S7), confirming the identity of these species and showing that LarE is responsible for sulfurization of P2CMN into P2TMN.

Role of CoA in LarE Activity. LC-ESI-MS profiles were then performed on LarE to identify the function of CoA in LarA cofactor biosynthesis. These profiles revealed that LarE (31,550 ± 1 Da for sample containing the StrepII-tag residues, ASWSHPQFEK, and missing the N-terminal Met) was accompanied by 119 ± 1 Da, 689 ± 1 Da, and 766 ± 1 Da larger species (*SI Appendix*, Fig. S8, *Top*). Analogous analysis of LarE purified in the presence of CoA provided a small amount of free protein and a large amount of species larger by 765 ± 1 Da. This species is consistent with a LarE-CoA mixed disulfide, and the 689 ± 1 Da version probably is

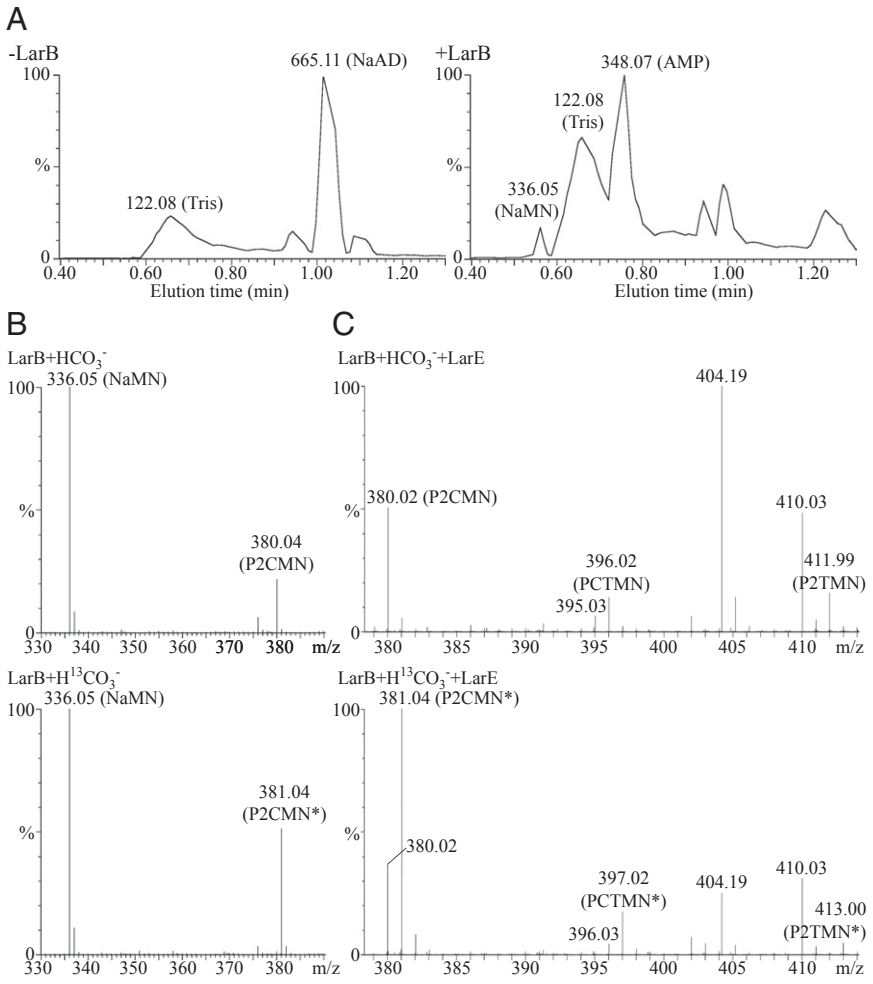

Fig. 2. Identification of the LarB and LarE products. (*A*) LC-ESI-MS chromatographs in positive-ionization mode of NaAD mixed with $MgCl_2$ (5 mM) and $NaHCO_3$ (10 mM) in the absence and presence of LarB. (*B*) Integration of the 0.5- to 0.6-min region of *A* with $NaHCO_3$ (10 mM) or $NaH^{13}CO_3$ (10 mM). (*C*) Integration of the 0.5- to 0.7-min region of a separate LC-ESI-MS chromatograph in positive-ionization mode after the LarE reaction with P2CMN or P2CMN*. The identities of the compounds as determined by LC-ESI-MS/MS (*SI Appendix*, Figs. S3, S6, and S7) are indicated next to the corresponding peaks, where the asterisk (*) indicates the presence of ^{13}C.

the same form after dephosphorylation (the 32,414 ± 1 Da species is attributable to contamination of the sample). LC-ESI-MS and MS/MS analysis of the tryptic digest of LarE confirmed the presence of CoA in disulfide linkage to Cys176 of LarE (*SI Appendix*, Fig. S9). In particular, a modified peptide of 1,659.51 Da was detected in both negative and positive ion ESI-MS modes that matches that expected for the mass of the peptide corresponding to residues 173–181 (894.41 Da) plus CoA (767.12 Da) less two protons (2.02 Da). Furthermore, several MS/MS products were consistent with this assignment, including some possessing a persulfide, as expected for fragmentation of a mixed disulfide (7) (*SI Appendix*, Fig. S9). We suggest the LarE-CoA disulfide is an off-pathway species likely to be formed by reaction of the nucleophilic LarE cysteinyl group with CoA disulfide formed in the aerobic solution (LarE-SH + CoA-S-S-CoA ↔ LarE-S-S-CoA + CoA-SH). Potentially, the P2CMN- and ATP-binding sites of LarE bind CoA to facilitate generation of the LarE-CoA mixed disulfide. This form may stabilize LarE in the absence of P2CMN. We propose that free CoA reduces LarE-CoA to provide the free protein that is needed for converting P2CMN to P2TMN.

Cysteine of LarE Is the Sulfur Donor. We next sought to identify the sulfur donor in the LarE reaction, for which the solution contained only purified LarC and LarE proteins and CoA as potential sulfur sources. Incubation of the LarB reaction mixture with LarE led to the transient development of a distinct LarE species (31,911 ± 1 Da, or 361 ± 1 Da larger than free LarE), followed by all LarE protein being converted to a 31,156 ± 1 species (34 Da less than LarE) by 45 min (Fig. 3*A* and *SI Appendix*, Fig. S8). The intermediate species increased by 1 mass unit when using $NaH^{13}CO_3$ in the LarB reaction solution, and the mass was consistent with LarE being linked to P2CMN (*SI Appendix*, Fig. S8). Neither the intermediate nor the final LarE species was observed in the absence of ATP (*SI Appendix*, Fig. S8), indicating that ATP is required for these transformations. The final LarE species, with a mass 34 Da smaller than the free protein, was shown to possess a peptide corresponding to residues 173–181 but with Cys replaced by dehydroalanine (Dha) (Fig. 3*B* and *SI Appendix*, Fig. S10). The loss of sulfur from Cys176 accompanies the conversion of P2CMN to P2TMN, consistent with LarE serving as a substrate by offering its cysteinyl group as the sulfur donor. Even though much of the protein begins as the CoA disulfide, all LarE is converted in this reaction because of the presence of excess CoA in the mixture (i.e., LarE-S-S-CoA + CoA-SH ↔ LarE-SH + CoA-S-S-CoA).

LarE purified from cells expressing the entire *larA-E* operon was mostly in the desulfurized form (*SI Appendix*, Fig. S11*A*), suggesting that the LarE cysteine is not regenerated in vivo. These results lead us to propose a reaction mechanism in which a carboxyl group of P2CMN is first adenylylated by ATP [similar to the activation of NaMN by the LarE homolog nicotinamide mononucleotide synthetase (8)], nucleophilic attack by Cys176 of LarE on the activated P2CMN leads to formation of the LarE-substrate adduct, and Dha176 formation is coupled to sulfur transfer and generation of PCTMN. Activation of the second carboxyl group, linkage to Cys176 of a second LarE protomer, and sulfur transfer then creates the final product P2TMN. Thus, two molecules of LarE undergo sacrificial sulfur transfer to create one P2TMN. This hypothesis is further supported by the observation that mutations of Asp30 of the pyrophosphatase (PP)-motif (9) and Cys176 inactivate LarE (*SI Appendix*, Fig. S11*B*) and by the

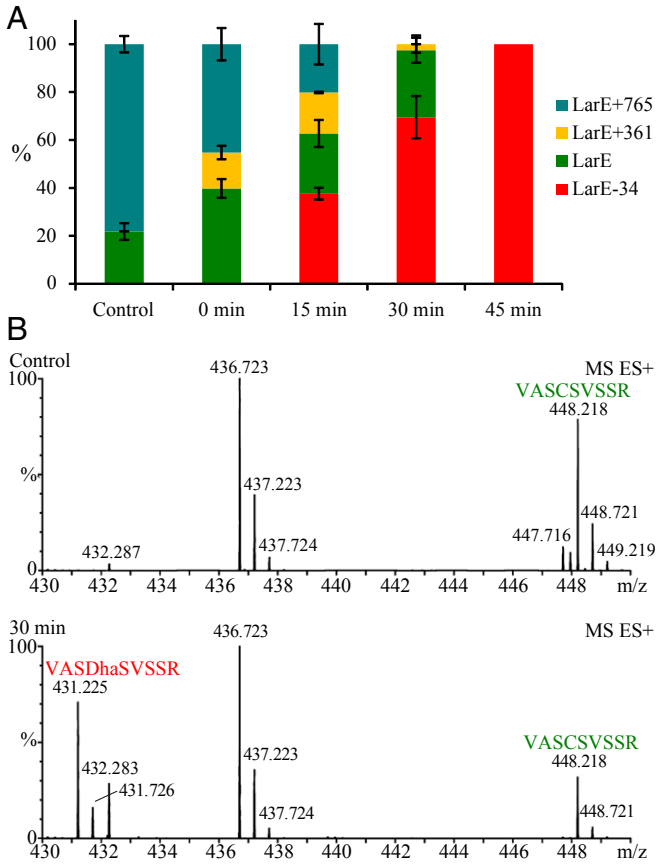

Fig. 3. Sulfur transfer from LarE to P2CMN. (*A*) Percentage of each form of LarE as observed by LC-MS-ESI before (Control) and 0, 15, 30, and 45 min after addition of the LarB product (*SI Appendix*, Fig. S8). Error bars represent the SD (n = 2). (*B*) LC-ESI-MS of a doubly charged tryptic peptide of LarE before (*Upper*) and 30 min after (*Lower*) addition of P2CMN. The sequences of the peptides analyzed by LC-ESI-MS/MS (*SI Appendix*, Fig. S10) are indicated above the corresponding peaks.

observation of a near 2:1 LarE:LarA ratio for optimal Lar activity (*SI Appendix*, Fig. S11*C*).

LarC-Mediated Nickel Insertion and Transfer to LarA. Further steps in the generation of Lar activity include nickel insertion into P2TMN, a process that must use LarC (which purifies with bound Ni) because nickel alone is not inserted (Fig. 4*A*), and transfer of the mature cofactor into the LarA apoprotein (3). We observed a time-dependent increase in Lar activity when the cofactor was transferred into *Lactobacillus plantarum* LarA apoprotein, requiring 90 min to reach maximal activity when sulfite, known to protect LarA from oxidation (1), was present (Fig. 4*B*). Our analysis of the in vitro-activated LarA proteins by LC-ESI-MS revealed the expected mass shift corresponding to the addition of the cofactor to LarA (*SI Appendix*, Fig. S12*A*). LC-ESI-MS and LC-ESI-MS/MS analyses of in vitro-activated LarA digested with trypsin confirmed the presence of K^{184}SVLPGIASYK peptide covalently linked to the (SCS)Ni(II) cofactor (*SI Appendix*, Figs. S12*B* and S13), as previously described (1). The mass of this peptide was shifted by 1 Da when using LarB-generated P2CMN* in the activation mixture (*SI Appendix*, Figs. S12*B* and S13), demonstrating that the cofactor in LarA is derived from P2TMN.

Discussion

We propose a scheme for the biosynthesis of active *L. plantarum* LarA in which LarB converts NaAD into P2CMN, LarE incorporates two sulfur atoms to yield P2TMN, LarC donates Ni, and the mature cofactor becomes covalently attached to LarA apoprotein (Fig. 5). The LarB-dependent carboxylation reaction requires bicarbonate/CO_2 (Fig. 1*C*) and somewhat resembles AIR carboxylation by the LarB homolog PurE (10); however, biological carboxylation of a pyridinium ring was previously unknown. To perform this chemistry, a nucleophilic amino acid of LarB may attack the pyridinium ring of NaAD to neutralize the positive charge and allow for direct attack of the ring C5 on CO_2. ATP is not required for the LarB reaction (Fig. 1*C*), so ATP-dependent activation of bicarbonate does not take place. An alternative hypothesis is that the LarB-catalyzed cleavage of the phosphoanhydride bond of NaAD may activate bicarbonate by formation of carboxy-AMP. This hypothesis would explain why NaMN is not a substrate of LarB (Fig. 1*C*).

LarE possesses multiple functions: activation of P2CMN by adenylylation, covalent linkage of the protein to P2CMN, sacrificial loss of its Cys176 sulfur atom to form the thioacid of P2CMN, and then repeating the set of reactions with a second LarE protomer to form P2TMN. Although we have not yet detected adenylylated P2CMN or the LarE-PCTMN derivative, we did observe the LarE-P2CMN adduct and demonstrated Dha in the product LarE. Sulfur-containing cofactors are typically synthesized by using the sulfur atom of free cysteine through the action of a persulfide-forming cysteine desulfurase (11); however, direct sulfur donation from a protein cysteinyl group, also generating a Dha residue, has been reported in the case of thiamine thiazole synthase of *Saccharomyces cerevisiae*, THI4p (12). Whereas a single molecule of THI4p is used to insert the lone sulfur atom

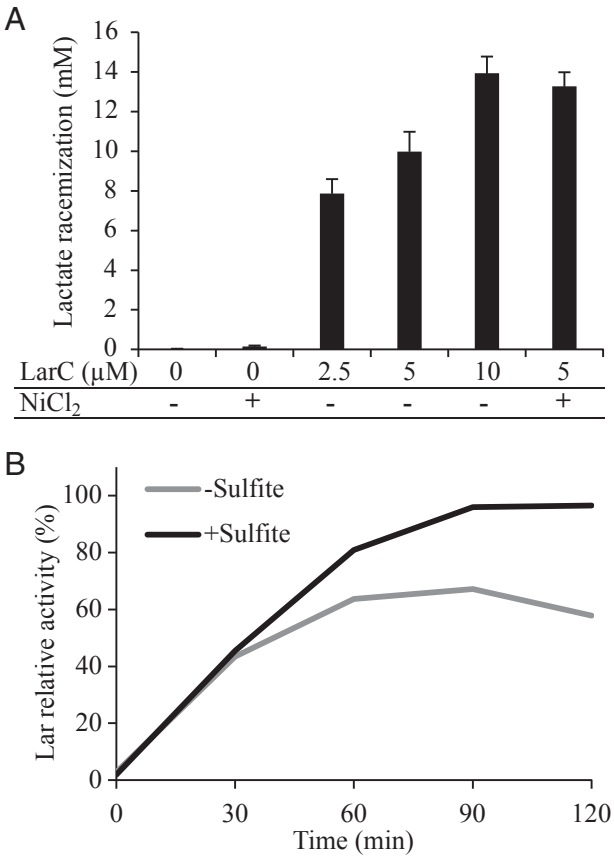

Fig. 4. LarC requirement and Lar activity generation. (*A*) Lar activity generated upon addition of LarA apoprotein to solutions incubated for 2 h with NaAD (0.5 mM), $NaHCO_3$ (10 mM), LarB (1 μM), LarE (5 μM), $MgCl_2$ (20 mM), ATP (5 mM), and CoA (1 mM) in Tris·HCl buffer (100 mM; pH 8) along with (where indicated) LarC and $NiCl_2$ (0.1 mM). (*B*) Time course of the in vitro activation of *L. plantarum* LarA in the absence (–Sulfite) or presence (+Sulfite) of 10 μM sulfite. Error bars represent the SD (n = 3).

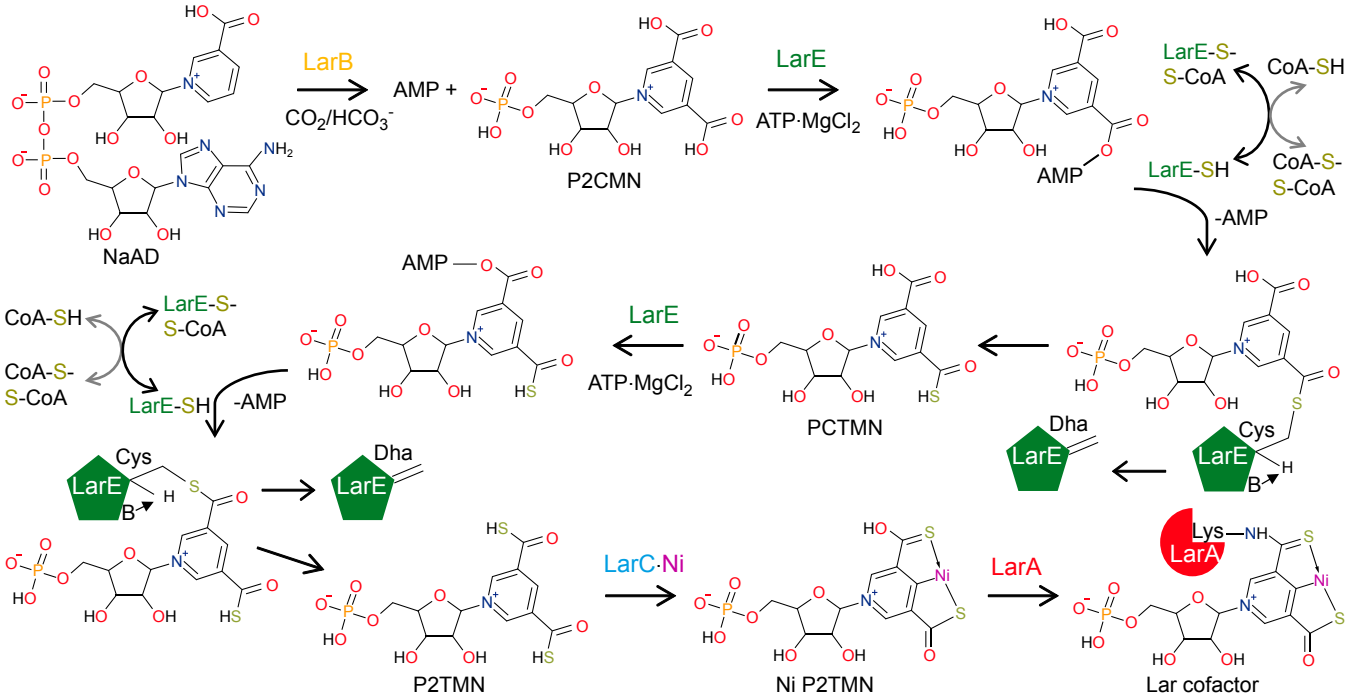

Fig. 5. Overall pathway for synthesis of the LarA cofactor.

needed for thiamine biosynthesis, two LarE molecules are needed as substrates for synthesis of P2TMN. Thus, synthesis of active LarA is very expensive for the cell by requiring two single-turnover LarE proteins per cofactor made. The steps involving Ni donation by LarC and covalent attachment of the cofactor to LarA have not been fully characterized, but LarE may be needed for both cofactor stabilization and to activate P2TMN for thioamide formation. Our studies have revealed key aspects of a previously unidentified biosynthetic pathway that transforms NaAD into the (SCS)Ni(II) pincer complex of LarA. This work paves the way to the isolation of the LarA cofactor and a better understanding of the chemical properties of this first, to our knowledge, biological pincer complex which, based on the prevalence of *larB*, *larC*, and *larE* homologs in other microorganisms, may participate in reactions other than lactate racemization (3).

Materials and Methods

Biological Materials and Growth Conditions. Bacterial strains and plasmids used in the present study are listed in *SI Appendix*, Table S1. We grew *Lactococcus lactis* in M17 broth supplemented with 0.5% glucose at 28 °C. $NiSO_4$ (1 mM) was added to cultures expressing pGIR051, and chloramphenicol (10 mg·L^{-1}) was provided when expressing plasmids derived from pNZ8048. For the induction of genes under control of the *nisA* expression signals, nisin A (Sigma-Aldrich) was added during the early exponential phase (OD_{600} = 0.3–0.4) at a concentration of 1 μg·L^{-1}, and the cells were collected after 4 h. *Escherichia coli* DH10B was grown with agitation (200 rpm) at 37 °C in LB containing erythromycin (200 mg·L^{-1}).

DNA Techniques. General molecular biology techniques were performed according to standard protocols (13). Transformation of *E. coli* and *L. lactis* was performed by electrotransformation (14, 15). PCR amplifications used Phusion high-fidelity DNA polymerase (New England Biolabs). The primers used in this study were purchased from IDT and are listed in *SI Appendix*, Table S1. Plasmid pGIR026, derived from pGIZ660 (4), bears a translational fusion of *larB* and DNA encoding the StrepII tag for expression in *E. coli*. pGIZ660 was PCR-amplified with the primers BT_A and BT_B, digested with NheI, and self-ligated, generating a 30-bp in-frame insertion of a fragment encoding the StrepII tag at the C terminus of LarB. The ligation mixture was treated with DpnI before transformation into *E. coli* to digest the original pGIZ660 plasmid template. Plasmids bearing variants of *larE* for expression in *L. lactis* were derived from pGIR072 (3) (i.e., pGIR072M1-M2) and provided the two variant forms (D30A, C176A) of LarE. For each construction, pGIR072 was first methylated by Dam methylase using *S*-adenosyl methionine (New England Biolabs), and PCR amplification was performed to obtain a fragment comprising the mutated plasmid. The PCR product was digested with DpnI before transformation in *L. lactis* according to the Quickchange mutagenesis protocol (16). The plasmid sequences were confirmed by sequencing with primer UP_PNZ8048′.

Cell Lysate Preparation. A total of 1.5 L of *L. lactis* cultures expressing pNZ8048 (empty vector) or pGIR022 (encoding LarB) were collected and the pellets were washed twice in 100 mM Tris·HCl at pH 7.5 (buffer T), resuspended in 15 mL of buffer T with 15 g·L^{-1} of lysozyme, incubated 30 min at 37 °C, and cooled 10 min on ice. This treatment was followed by sonication at maximum amplitude (Branson Sonifier 450) using two series of 10 one-second pulses with an intervening 1-min pause on ice. Clear supernatants were obtained after centrifugation at 12,000 × *g* for 25 min at 4 °C. For obtaining deproteinized cell lysates, the supernatants were placed into an Amicon Ultra-15 centrifugal filter unit (10-kDa cutoff; Merck Millipore) and spun, and the flow-through fraction was collected.

Protein Purification. LarA from *L. plantarum* ($LarA_{Lp}$) or *Thermoanaerobacterium thermosaccharolyticum* ($LarA_{Tt}$), LarC, and LarE were purified from 1.5 L of the appropriate *L. lactis* cultures (containing plasmids that are listed in *SI Appendix*, Table S1), which were collected by centrifugation (5,000 × *g* for 10 min) and washed twice with 50 mL of 100 mM Tris·HCl (pH 7.5) buffer containing 150 mM NaCl (buffer W). Cells were resuspended in 15 mL of W buffer and transferred by 0.5-mL aliquots into 0.5-mL suspensions of glass beads (≤106 μm; Sigma) in W buffer using 2-mL microtubes. Lysis was accomplished by using a Mini-Beadbeater-16 (BioSpec Products) twice for 1-min periods, with 2 min of cooling on ice between the runs. After lysis, the soluble fractions were collected by centrifugation at 20,000 × *g* for 15 min at 4 °C. Affinity chromatography was performed with gravity-flow Strep-Tactin Superflow high-capacity columns of 1.5 mL, as described (17), with buffer W. For purification of LarE in the presence or CoA, 0.5 mM CoA was added to all buffers. Protein concentrations were measured by Bradford assay (18).

LarB was purified from 1.5 L of overnight *E. coli* culture expressing pGIR026. The cells were collected, and the pellet was washed twice in buffer W, resuspended in buffer W with 1 g·L^{-1} lysozyme, incubated for 30 min at 37 °C, and cooled for 10 min on ice. This treatment was followed by sonication at maximum amplitude (Branson Sonifier 450) using three series of 10 one-second pulses with intervening 2-min pauses on ice. Clear supernatant was obtained after centrifugation at 12,000 × *g* for 30 min at 4 °C. Affinity

chromatography was performed with gravity-flow Strep-Tactin Superflow high-capacity columns of 1.5 mL, as described (17), with buffer W.

In Vitro Activation of LarA by Lysates from LarB-Containing Cells or by Purified LarB, LarC, and LarE. We incubated a mixture of LarE (5 μM), LarC (5 μM), ATP (5 mM), $MgCl_2$ (20 mM), and CoA (1 mM) in Tris·HCl buffer (100 mM; pH 8) with 10 μL of lysates from *lar*-free cells or cells expressing *larB* in a final volume of 20 μL. After 1 h of incubation at room temperature (RT), 5 μL of the assay mixture was diluted into 45 μL of L-lactate (45 mM) supplemented with $LarA_{Tt}$ apoprotein (0.8 μM) in Hepes buffer (100 mM; pH 7). The reaction was incubated for 5 min at 50 °C and then stopped by heat treatment at 90 °C. The resulting D-lactate concentration was measured by enzymatic lactate oxidation to pyruvate using a D-lactic acid/L-lactic acid commercial test (Megazyme), as previously described (3). The NADH absorbance was monitored at 340 nm with a SpectraMax M5 (Molecular Devices) (*SI Appendix*, Fig. S1). For optimization of $MgCl_2$, ATP, and CoA concentrations, the concentration of one component was varied with the other components held static. For analyses of LC fractions, the lysates were replaced by LarB reaction products (control) or by LC-separated fractions of LarB reaction products (*SI Appendix*, Fig. S2).

To examine the purified LarB reaction, we replaced the lysate in the previous experiment with LarB (1 μM) and incubated it with NaMN (0.5 mM) or NaAD (0.5 mM) along with $NaHCO_3$ (10 mM) and $NiCl_2$ (0.1 mM). After 2 h of incubation at RT, L-lactate (45 mM) supplemented with $LarA_{Tt}$ apoprotein (0.8 μM) was added, and Lar activity was measured as described above in Fig. 1*B*. For analyses of LarE variants, LarE was replaced by D30A LarE and C176A LarE (*SI Appendix*, Fig. S11*B*). For analyses of LarC activity, LarC was added at different concentrations (Fig. 4*A*). For analysis of the separate LarB carboxylation reaction, LarB (0.5 μM) was mixed with NaMN (0.2 mM), NaAD (0.2 mM), $NaHCO_3$ (100 mM), ATP (5 mM), $NiCl_2$ (0.1 mM), and $MgCl_2$ (4 mM) in Tris·HCl buffer (100 mM; pH 8) and incubated 10 min at RT, and the reaction stopped by heat treatment at 90 °C. The reaction solutions were used instead of the cell lysate for in vitro activation of $LarA_{Tt}$, as described above in Fig. 1*C*. For optimization of the LarB carboxylation reaction, LarB (0.5 μM) was mixed with varied concentrations of one component with the other components held static [NaAD (0.2 mM), $NaHCO_3$ (50 mM), and $MgCl_2$ (4 mM) in Tris·HCl buffer (100 mM; pH 8)], incubated 5 min at RT, and the reaction was stopped by heat treatment at 90 °C. The reaction solutions were used for in vitro activation of $LarA_{Tt}$, as described above in *SI Appendix*, Fig. S4. For measurement of the concentrations of AMP released from NaAD, the AMP-Glo Assay (Promega) was used (*SI Appendix*, Fig. S5). For studying the properties of phosphoanhydride cleavage by LarB, the NaAD, $NaHCO_3$, and $MgCl_2$ concentrations were modified as indicated.

LC-ESI-MS of Small Molecules. For LC-ESI-MS analysis of the LarB product, we incubated LarB (5 μM), NaAD (0.5 mM), $MgCl_2$ (4 mM), and $NaHCO_3$ (10 mM) or $NaH^{13}CO_3$ (10 mM) in Tris·HCl buffer (100 mM; pH 8) in a final volume of 250 μL. After overnight incubation, samples were analyzed directly by LC-ESI-MS (Fig. 2 *A* and *B*). For analysis of the LarE product (Fig. 2*C*), we incubated the product of the previous LarB reaction with LarE (15 μM), ATP (5 mM), $MgCl_2$ (20 mM), and CoA (1 mM) in a final volume of 250 μL, concentrated the sample after a 30-min reaction at RT to 50 μL in an Amicon Ultra-0.5 (10 kDa cutoff) centrifugal filter (Merck Millipore), and washed the product three times with ammonium bicarbonate (AB) buffer (100 mM; pH 8). Trypsin (5 μg) was added, the protein was digested for 2 h at 37 °C, and samples were analyzed by LC-ESI-MS. For analysis of small molecules, 10-μL aliquots were injected into a Waters Acquity ultra-performance LC system coupled to a Waters Xevo G2-S quadruple time-of-flight mass spectrometer. Separations were performed using a bridged ethylene hybrid (BEH) C18 (100 mm × 2.1 mm; 1.7-μm particle size) column with an isocratic flow of 10 mM AB buffer (pH 8) at 30 °C. The run time for each sample was 15 min. MS/MS spectra (*SI Appendix*, Figs. S6 and S7) were generated by using argon as collision gas and a collision cell potential 10 V.

LC-ESI-MS of Proteins and Peptides. For analysis of the different forms of LarE (Fig. 3*A* and *SI Appendix*, Figs. S8 and S11), LarE (10 μM) was incubated with ATP (5 mM), $MgCl_2$ (20 mM), and 50% volume of LarB reaction (as described for LC-ESI-MS of LarB product) for 0, 15, 30, and 45 min and analyzed by LC-ESI-MS; 10-μL aliquots were injected into the UPLC system coupled to the QTof mass spectrometer. Separations were performed on a BetaBasic CN (10 mm × 1 mm; 5-μm particle size) column with an aqueous phase of 0.1% formic acid and using a gradient of increasing acetonitrile at 30 °C. The run time for each sample was 15 min. The masses were calculated from the ESI-MS spectrum using the advanced maximum entropy (MaxEnt)-based procedure included in the Micromass MassLynx software package.

For LC-ESI-MS analysis of peptides (Fig. 3*B* and *SI Appendix*, Figs. S9 and S10), LarE (100 μg) was digested with trypsin (5 μg) for 2 h at 37 °C; 10-μL aliquots were injected into the UPLC system coupled to the QTof mass spectrometer. Separations were performed on a BEH C18 (100 mm × 2.1 mm; 1.7-μm particle size) column with an aqueous phase of 0.1% formic acid and a gradient of increasing acetonitrile at 40 °C. The run time for each sample was 15 min. MS/MS spectra were generated by using argon as the collision gas and a collision cell potential of 40 V.

$LarA_{Lp}$ Apoprotein in Vitro Activation. We incubated LarB (1 μM), LarE (10 μM), LarC (10 μM), NaAD (0.5 mM), ATP (5 mM), $MgCl_2$ (20 mM), CoA (1 mM), $NaHCO_3$ (10 mM), and $NiCl_2$ (0.1 mM) in Tris·HCl buffer (100 mM; pH 8) in a final volume of 25 μL for 2 h at RT. $LarA_{Lp}$ in vitro activation was started by adding apoprotein (6 μM) in Tris·HCl buffer (100 mM; pH 8) in a final volume of 50 μL. The sample was activated for 30 min at RT, and 3 μL was diluted into 47 μL of 45 mM L-lactate in Hepes (100 mM; pH 7) buffer to measure Lar activity. For the time-course experiment (Fig. 4*B*), we used $LarA_{Lp}$ in Hepes buffer (400 mM; pH 7), and Na_2SO_3 (10 μM) was added where indicated. The assay was incubated for 0, 30, 60, 90, and 120 min at RT, and 3 μL was diluted into 47 μL of 45 mM L-lactate in Mes (100 mM; pH 6) buffer. The reaction was incubated for 5 min at 35 °C and stopped by heat treatment at 90 °C, and the Lar activity was measured as described above. For LC-ESI-MS analysis, 250 μL of the LarA in vitro activation mixture (incubated for 90 min at RT) was directly analyzed (*SI Appendix*, Fig. S12*A*) or washed three times with AB buffer (100 mM; pH 8), trypsin-digested as described previously (1), and analyzed (*SI Appendix*, Figs. S12*B* and S13).

ACKNOWLEDGMENTS. We thank the Michigan State University Mass Spectrometry and Metabolomics Core for data collection. This work was supported by National Science Foundation Grant CHE-1516126 (to R.P.H.), Michigan State University (R.P.H.), the Belgian National Fund for Scientific Research (FNRS) (P.H. and P.S.), and the Université catholique de Louvain-Fonds Spéciaux de Recherche (P.H. and P.S.).

1. Desguin B, et al. (2015) A tethered niacin-derived pincer complex with a nickel-carbon bond in lactate racemase. *Science* 349(6243):66–69.
2. Xu T, Bauer G, Hu X (2016) A novel nickel pincer complex in the active site of lactate racemase. *ChemBioChem* 17(1):31–32.
3. Desguin B, et al. (2014) Lactate racemase is a nickel-dependent enzyme activated by a widespread maturation system. *Nat Commun* 5:3615.
4. Goffin P, et al. (2005) Lactate racemization as a rescue pathway for supplying D-lactate to the cell wall biosynthesis machinery in *Lactobacillus plantarum*. *J Bacteriol* 187(19):6750–6761.
5. Gazzaniga F, et al. (2009) Microbial NAD metabolism: Lessons from comparative genomics. *Microbiol Molec Biol Rev* 73(3):529–541.
6. Tranchimand S, Starks CM, Mathews II, Hockings SC, Kappock TJ (2011) *Treponema denticola* PurE is a bacterial AIR carboxylase. *Biochemistry* 50(21):4623–4637.
7. Wang Z, Rejtar T, Zhou ZS, Karger BL (2010) Desulfurization of cysteine-containing peptides resulting from sample preparation for protein characterization by mass spectrometry. *Rapid Commun Mass Spectrom* 24(3):267–275.
8. Sorci L, et al. (2009) Nicotinamide mononucleotide synthetase is the key enzyme for an alternative route of NAD biosynthesis in *Francisella tularensis*. *Proc Natl Acad Sci USA* 106(9):3083–3088.
9. Bork P, Koonin EV (1994) A P-loop-like motif in a widespread ATP pyrophosphatase domain: Implications for the evolution of sequence motifs and enzyme activity. *Proteins* 20(4):347–355.
10. Kappock TJ, Ealick SE, Stubbe J (2000) Modular evolution of the purine biosynthetic pathway. *Curr Opin Chem Biol* 4(5):567–572.
11. Black KA, Dos Santos PC (2015) Shared-intermediates in the biosynthesis of thiocofactors: Mechanism and functions of cysteine desulfurases and sulfur acceptors. *Biochim Biophys Acta* 1853(6):1470–1480.
12. Chatterjee A, et al. (2011) *Saccharomyces cerevisiae* THI4p is a suicide thiamine thiazole synthase. *Nature* 478(7370):542–546.
13. Sambrook J, Fritsch E, Maniatis T (1989) *Molecular Cloning: A Laboratory Manual* (Cold Spring Harbor Laboratory Press, New York), 2nd Ed.
14. Holo H, Nes IF (1989) High-frequency transformation, by electroporation, of *Lactococcus lactis* subsp. *cremoris* grown with glycine in osmotically stabilized media. *Appl Environ Microbiol* 55(12):3119–3123.
15. Dower WJ, Miller JF, Ragsdale CW (1988) High efficiency transformation of *E. coli* by high voltage electroporation. *Nucleic Acids Res* 16(13):6127–6145.
16. Zheng L, Baumann U, Reymond JL (2004) An efficient one-step site-directed and site-saturation mutagenesis protocol. *Nucleic Acids Res* 32(14):e115.
17. Schmidt TG, Skerra A (2007) The Strep-tag system for one-step purification and high-affinity detection or capturing of proteins. *Nat Protoc* 2(6):1528–1535.
18. Bradford MM (1976) A rapid and sensitive method for the quantitation of microgram quantities of protein utilizing the principle of protein-dye binding. *Anal Biochem* 72: 248–254.

SUPPLEMENTARY INFORMATION

Nickel-pincer cofactor biosynthesis involves LarB-catalyzed pyridinium carboxylation and LarE-dependent sacrificial sulfur insertion

Benoît Desguin, Patrice Soumillion, Pascal Hols & Robert P. Hausinger

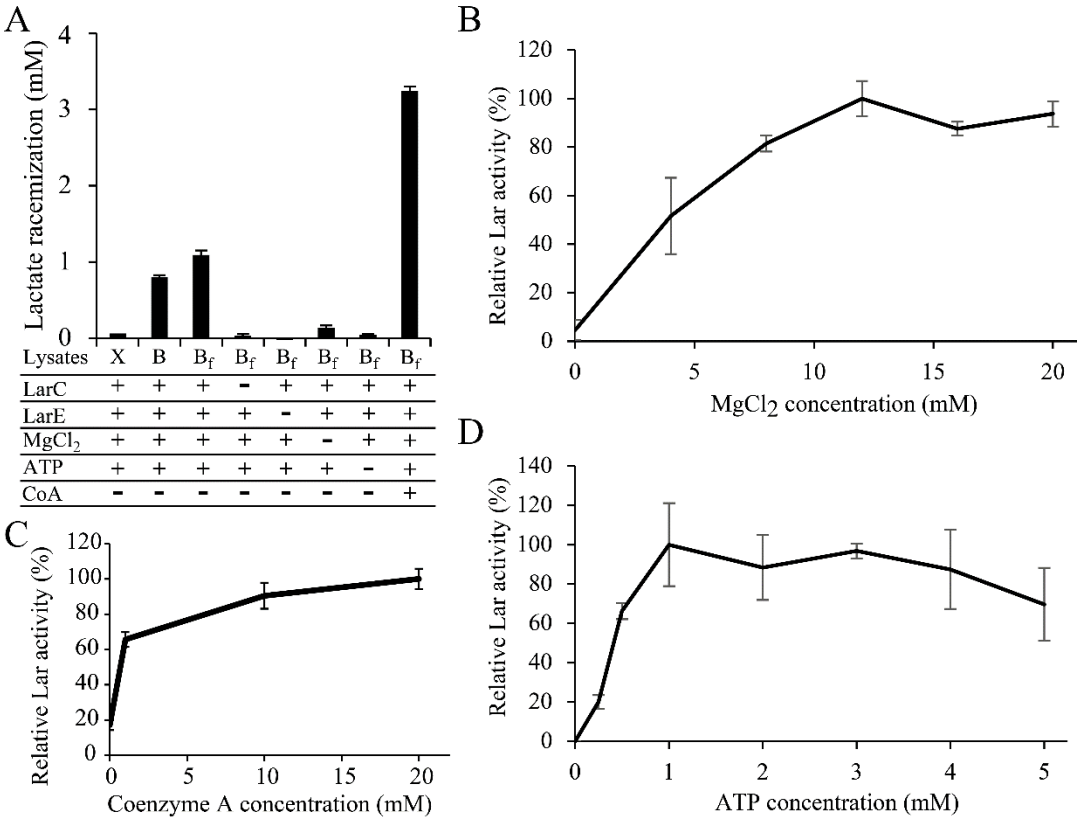

Fig. S1. *In vitro* activation of LarA using lysates from LarB-containing cells. (**A**) Lar activity generated upon addition of LarA apoprotein to solutions incubated for 1 h with the LarE (5 µM), LarC (5 µM), $MgCl_2$ (20 mM), ATP (5 mM) and CoA (1 mM) in Tris-HCl buffer (100 mM, pH 8) along with 50% V/V lysates from *lar*-free cells (X), lysates from cells expressing *larB* (B), or ultrafiltered lysates from cells expressing *larB* (B_f). Concentration

dependence of (**B**) $MgCl_2$, (**C**) ATP, and (**D**) CoA in the *in vitro* LarA activation reaction with 50 % V/V lysates from cells expressing *larB*. 100% Lar activity is that obtained for a LarE + LarC reaction containing 12 mM $MgCl_2$, 1 mM ATP and 20 mM CoA, respectively. Error bars represent the SD (N=3).

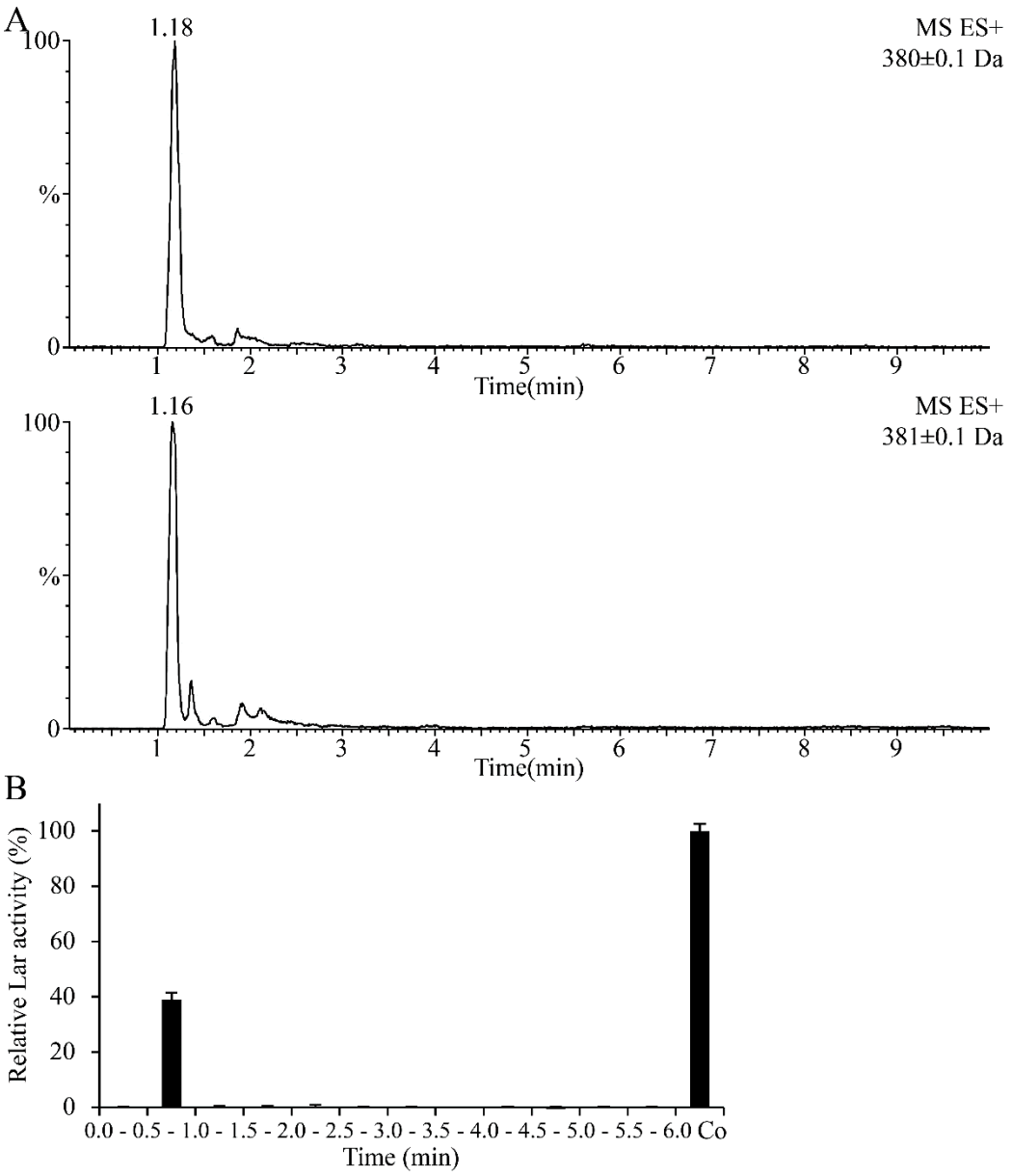

Fig. S2. LC of the LarB product. (**A**) Retention time of the *m/z* 380 species (top) and *m/z* 381 species (bottom) of the LarB *in vitro* reaction with $NaHCO_3$ (top) and $NaH^{13}CO_3$ (bottom) in positive ionization mode. The ordinate represents the abundance relative to the highest peak in %. (**B**) Relative Lar activity of LarA *in vitro* activation with the 0.5 min-6.5 min fractions of the LarB *in vitro* reaction after LC as in **A**. 100% activity is the Lar activity of the sample before injection (Co). Error bars represent the SD (N=4).

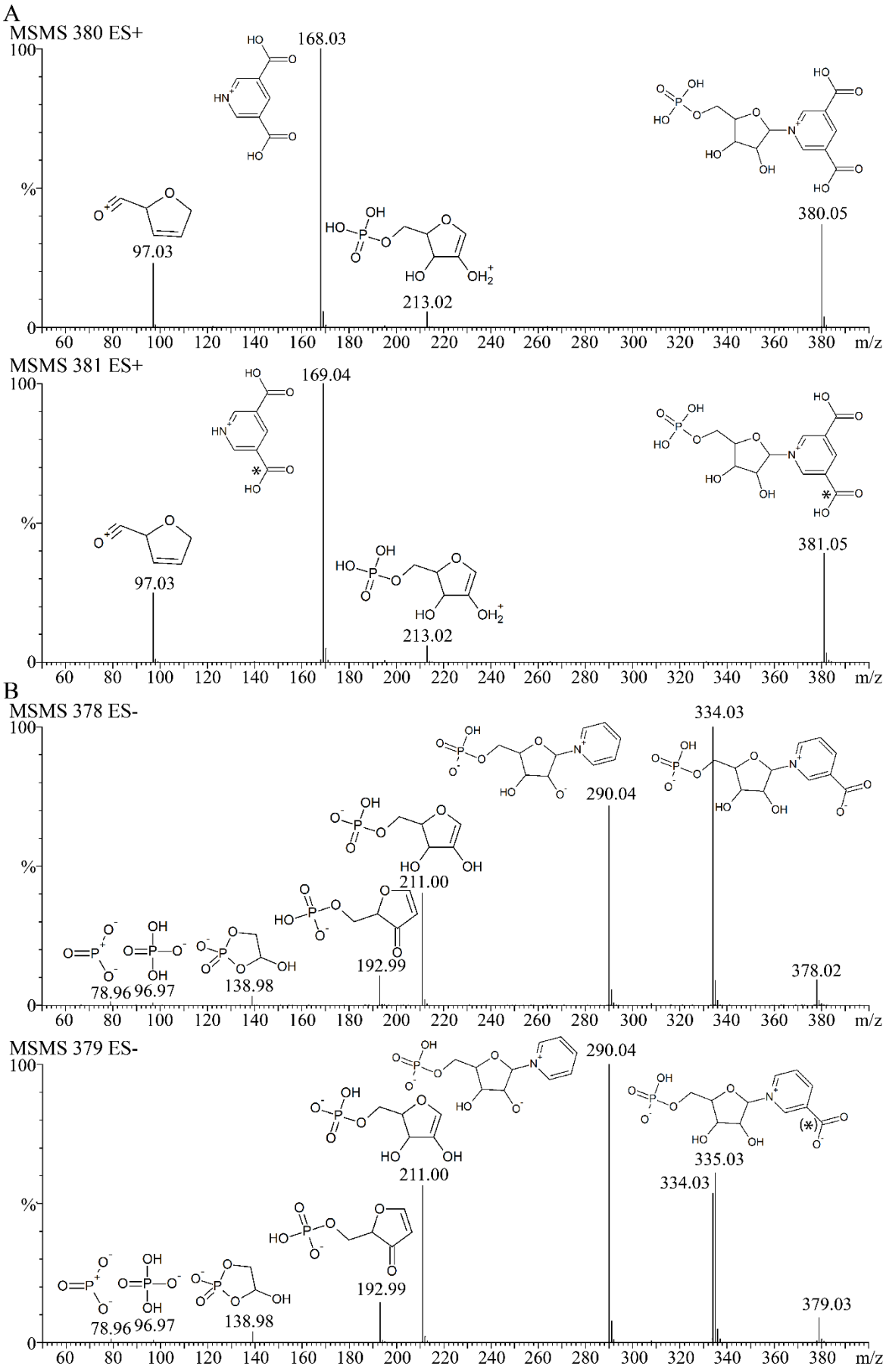
A
MSMS 380 ES+
100
%
0
168.03
97.03
213.02
380.05
60 80 100 120 140 160 180 200 220 240 260 280 300 320 340 360 380 m/z
MSMS 381 ES+
100
%
0
169.04
97.03
213.02
381.05
60 80 100 120 140 160 180 200 220 240 260 280 300 320 340 360 380 m/z
B
MSMS 378 ES-
100
%
0
334.03
290.04
211.00
192.99
78.96
96.97
138.98
378.02
60 80 100 120 140 160 180 200 220 240 260 280 300 320 340 360 380 m/z
MSMS 379 ES-
100
%
0
290.04
211.00
335.03
334.03
192.99
78.96
96.97
138.98
379.03
60 80 100 120 140 160 180 200 220 240 260 280 300 320 340 360 380 m/z

Fig. S3. MS/MS Fragmentation of P2CMN. LC-ESI-MS/MS fragmentation in positive (**A**) and negative (**B**) ionization mode of the 379 Da (top) and 380 Da (bottom) species from the *in vitro* LarB reaction with $NaHCO_3$ (top) and $NaH^{13}CO_3$ (bottom). The ordinate represents the abundance relative to the highest peak in %. Possible structures of the fragments are drawn next to the corresponding peaks of the spectra. A "*" indicates the presence of ^{13}C, while "(*)" indicates a 50% probability of ^{13}C. The species at *m/z* 335.03 also contains the +1 isotopic species of the species at *m/z* 334.03, which explains why the species at *m/z* 335.03 is slightly more intense than the species at *m/z* 334.03.

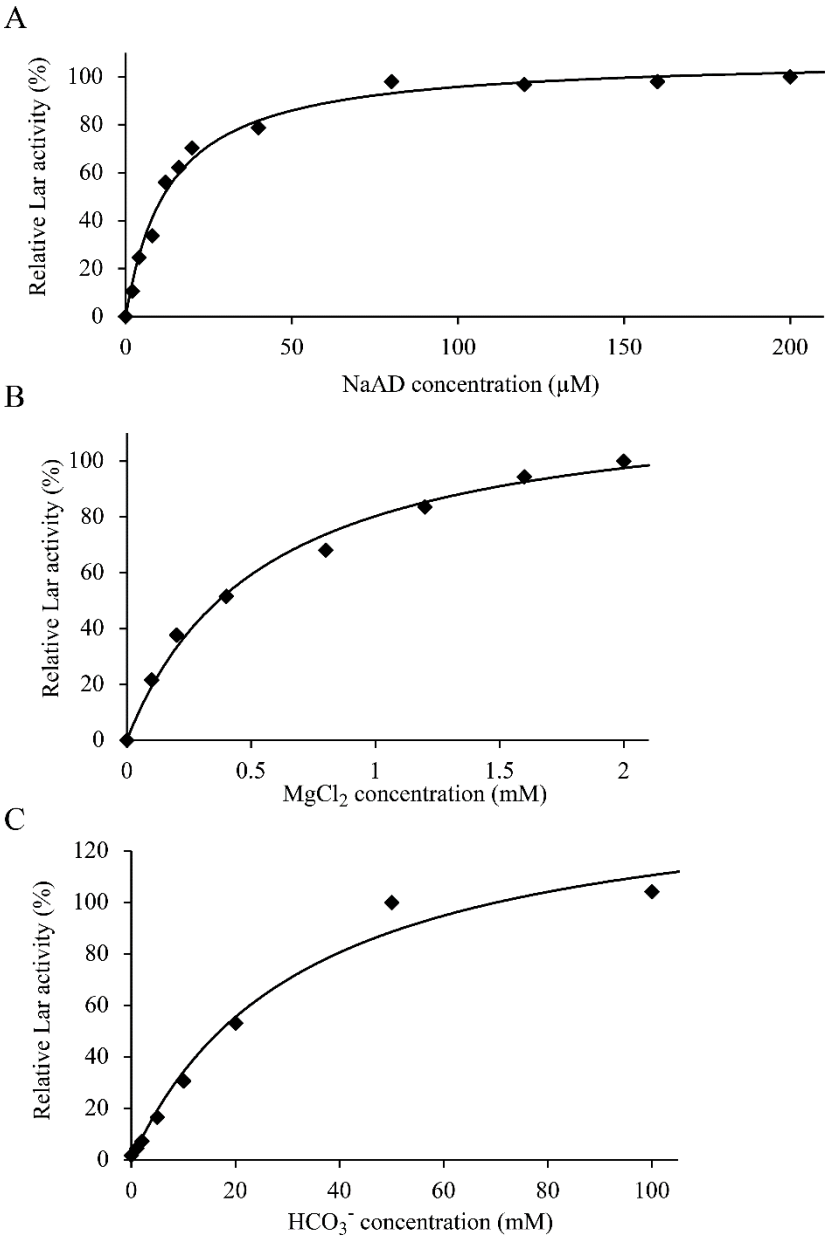

Fig. S4. Properties of the LarB *in vitro* carboxylation reaction as assessed by Lar activity. Concentration dependence of (**A**) NaAD, (**B**) $MgCl_2$, and (**C**) $NaHCO_3$ in the *in vitro* LarB reaction followed by *in vitro* activation of LarA. The non-variable concentrations for NaAD, $MgCl_2$, and $NaHCO_3$ are 200 μM, 4 mM, and 50 mM, and 100% Lar activity is that obtained for a LarB reaction containing these concentrations. Symbols represent the average of four replicates; fitted curves are calculated by non-linear least squares regression using the equation $v_0 = \frac{V_{\max}[S]}{K_m+[S]}$.

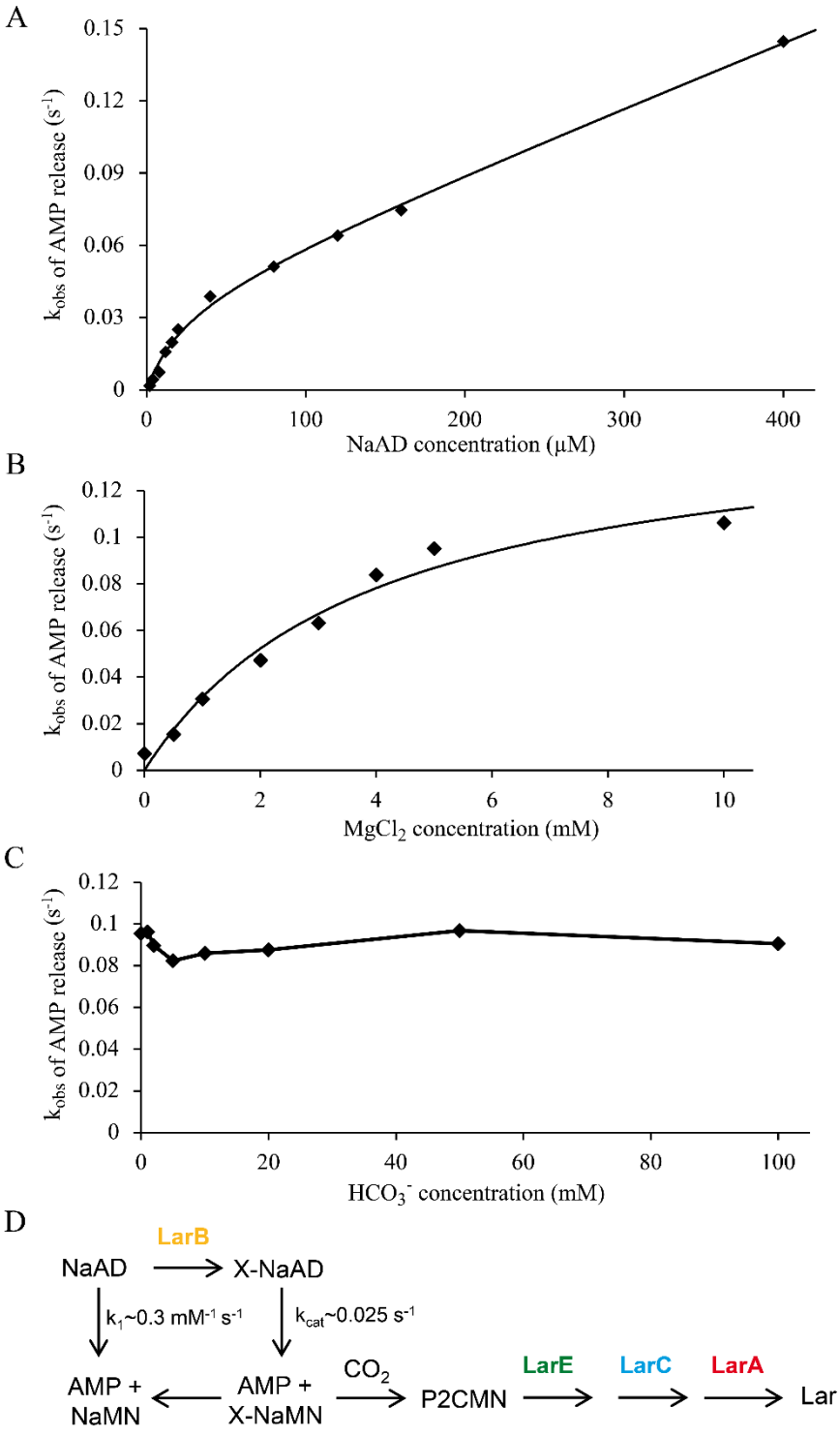

Fig. S5. Properties of the LarB *in vitro* hydrolysis reaction as assessed by AMP release. Concentration dependence of (**A**) NaAD, (**B**) $MgCl_2$, and (**C**) $NaHCO_3$ in the *in vitro* LarB reaction as followed by using an assay for AMP. The non-variable concentrations for NaAD, $MgCl_2$, and $NaHCO_3$ are 200 μM, 4 mM, and 50 mM. The observed NaAD hydrolysis rate

constants were estimated by dividing the rate of AMP appearance by the concentration of the LarB protein. Symbols represent the average of three replicates; fitted curves in **A** and **B** are calculated by non-linear least squares regression using the equations $k_{\mathrm{obs}} = \frac{k_{\mathrm{cat}}[\mathrm{S}]}{K_{\mathrm{m}}+[\mathrm{S}]} + k_{\mathrm{l}}[S]$ and $k_{\mathrm{obs}} = \frac{k_{\mathrm{cat}}[\mathrm{S}]}{K_{\mathrm{m}}+[\mathrm{S}]}$, respectively.(**D**) Scheme depicting the potential reaction kinetics of LarB as measured by Lar activity and AMP release where X is a nucleophile of the enzyme.

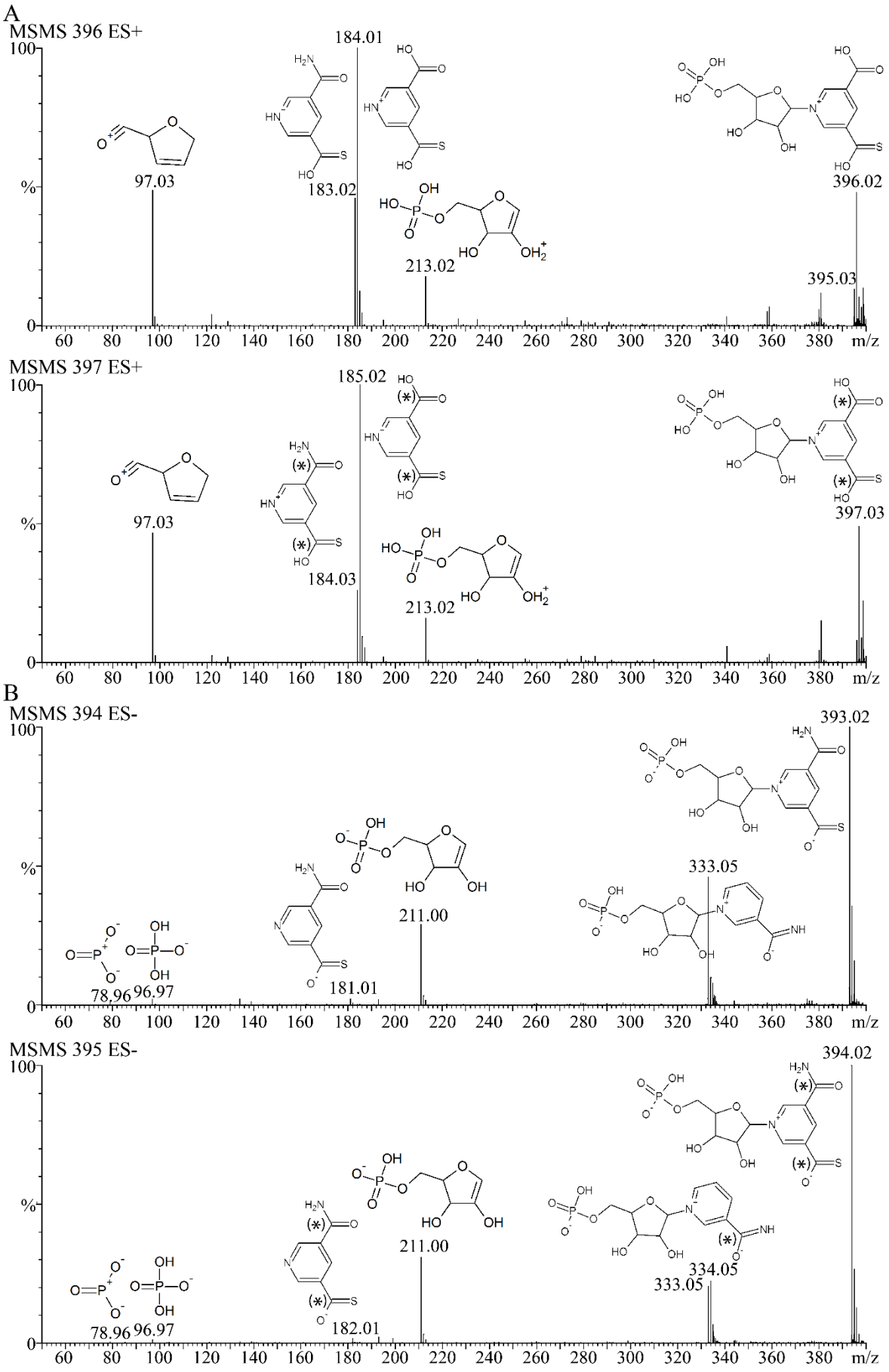
A
MSMS 396 ES+
184.01
97.03
183.02
213.02
396.02
395.03
MSMS 397 ES+
185.02
97.03
184.03
213.02
397.03
B
MSMS 394 ES-
393.02
211.00
333.05
78.96
96.97
181.01
MSMS 395 ES-
394.02
211.00
334.05
333.05
78.96
96.97
182.01
100
%
0
60 80 100 120 140 160 180 200 220 240 260 280 300 320 340 360 380 m/z

Fig. S6. MS/MS Fragmentation of PCTMN. LC-ESI-MS/MS fragmentation in positive (**A**) and negative (**B**) ionization mode of the 395 Da (top) and 396 Da (bottom) species after tryptic digestion of the *in vitro* reaction of LarE with P2CMN (top) and P2CMN* (bottom). The ordinate represents the abundance relative to the highest peak in %. Possible structures of the fragments are shown next to the corresponding peaks of the spectra. A "*" indicates the presence of ^{13}C, while "(*)" indicates 50% probability of ^{13}C.

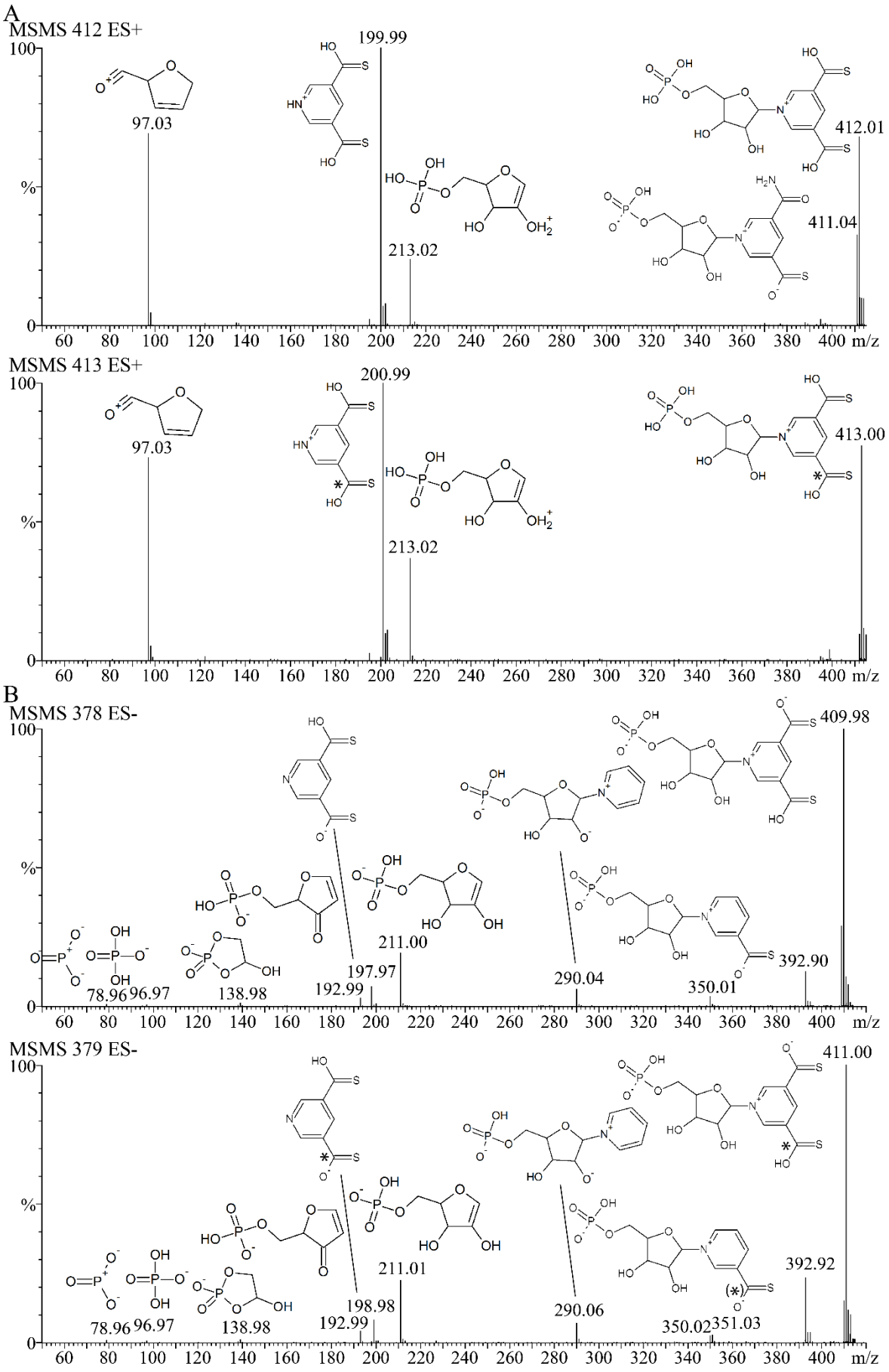
A
MSMS 412 ES+
199.99
97.03
412.01
411.04
213.02
MSMS 413 ES+
200.99
97.03
413.00
213.02
B
MSMS 378 ES-
409.98
211.00
197.97
290.04
392.90
350.01
78.96
96.97
138.98
192.99
MSMS 379 ES-
411.00
211.01
198.98
290.06
392.92
350.02
351.03
78.96
96.97
138.98
192.99
100
%
0
60 80 100 120 140 160 180 200 220 240 260 280 300 320 340 360 380 400 m/z

Fig. S7. MS/MS Fragmentation of P2TMN. LC-ESI-MS/MS fragmentation in positive (**A**) and negative (**B**) ionization mode of the 411 Da (top) and 412 Da (bottom) species after tryptic digestion of the *in vitro* reaction LarE with P2CMN (top) and P2CMN* (bottom). The ordinate represents the abundance relative to the highest peak in %. Possible structures of the fragments are shown next to the corresponding peaks of the spectra. A "*" indicates the presence of ^{13}C, while "(*)" indicates 50% probability of ^{13}C.

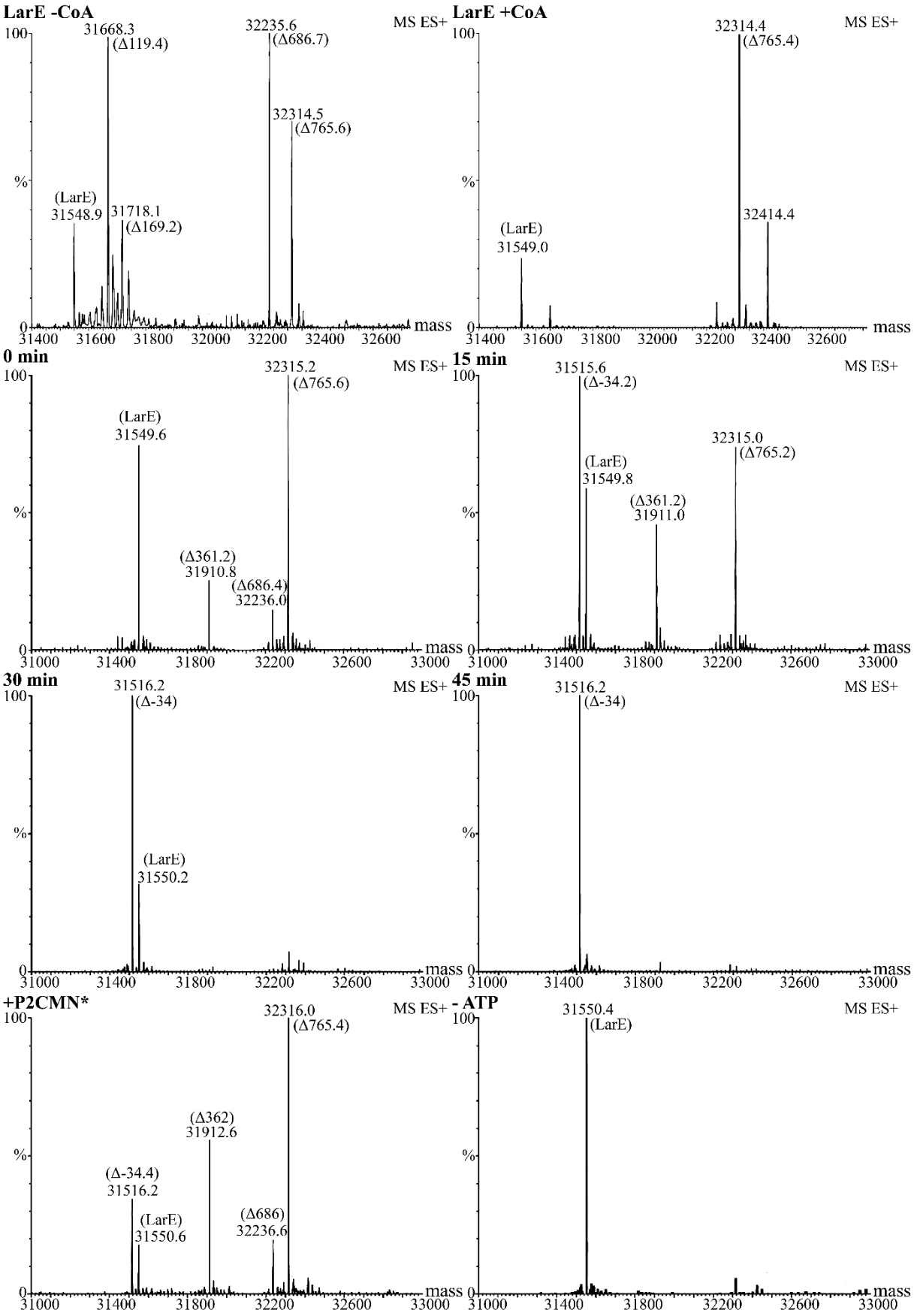
LarE -CoA
MS ES+
31668.3
(Δ119.4)
32235.6
(Δ686.7)
32314.5
(Δ765.6)
(LarE)
31548.9
31718.1
(Δ169.2)
mass
LarE +CoA
MS ES+
32314.4
(Δ765.4)
(LarE)
31549.0
32414.4
mass
0 min
MS ES+
32315.2
(Δ765.6)
(LarE)
31549.6
(Δ361.2)
31910.8
(Δ686.4)
32236.0
mass
15 min
MS ES+
31515.6
(Δ-34.2)
32315.0
(Δ765.2)
(LarE)
31549.8
(Δ361.2)
31911.0
mass
30 min
MS ES+
31516.2
(Δ-34)
(LarE)
31550.2
mass
45 min
MS ES+
31516.2
(Δ-34)
mass
+P2CMN*
MS ES+
32316.0
(Δ765.4)
(Δ362)
31912.6
(Δ-34.4)
31516.2
(LarE)
31550.6
(Δ686)
32236.6
mass
- ATP
MS ES+
31550.4
(LarE)
mass

Fig. S8. LC-ESI-MS profiles of LarE prior to and during its *in vitro* reaction. (**Top row**) Masses of LarE purified without (LarE -CoA) and with CoA (LarE +CoA) as observed in positive ionization mode. (**Middle 2 rows**) LarE masses as observed by LC-MS-ESI in positive ionization mode examined at 0, 15, 30, and 45 min after addition of the optimized *in vitro* LarB reaction solution (0, 15, 30 and 45 min). (**Bottom row, left**) LarE masses 15 min after addition of the *in vitro* LarB reaction solution prepared with $NaH^{13}CO_3$ (+P2CMN*). (**Bottom row, right**) LarE masses 30 min after addition of the LarB reaction solution following treatment with apyrase (-ATP). In each case, the ordinate represents the abundance relative to the highest peak in %. The numbers in parentheses indicate the mass difference from LarE (StrepII-tagged and minus the *N*-terminal methionine).

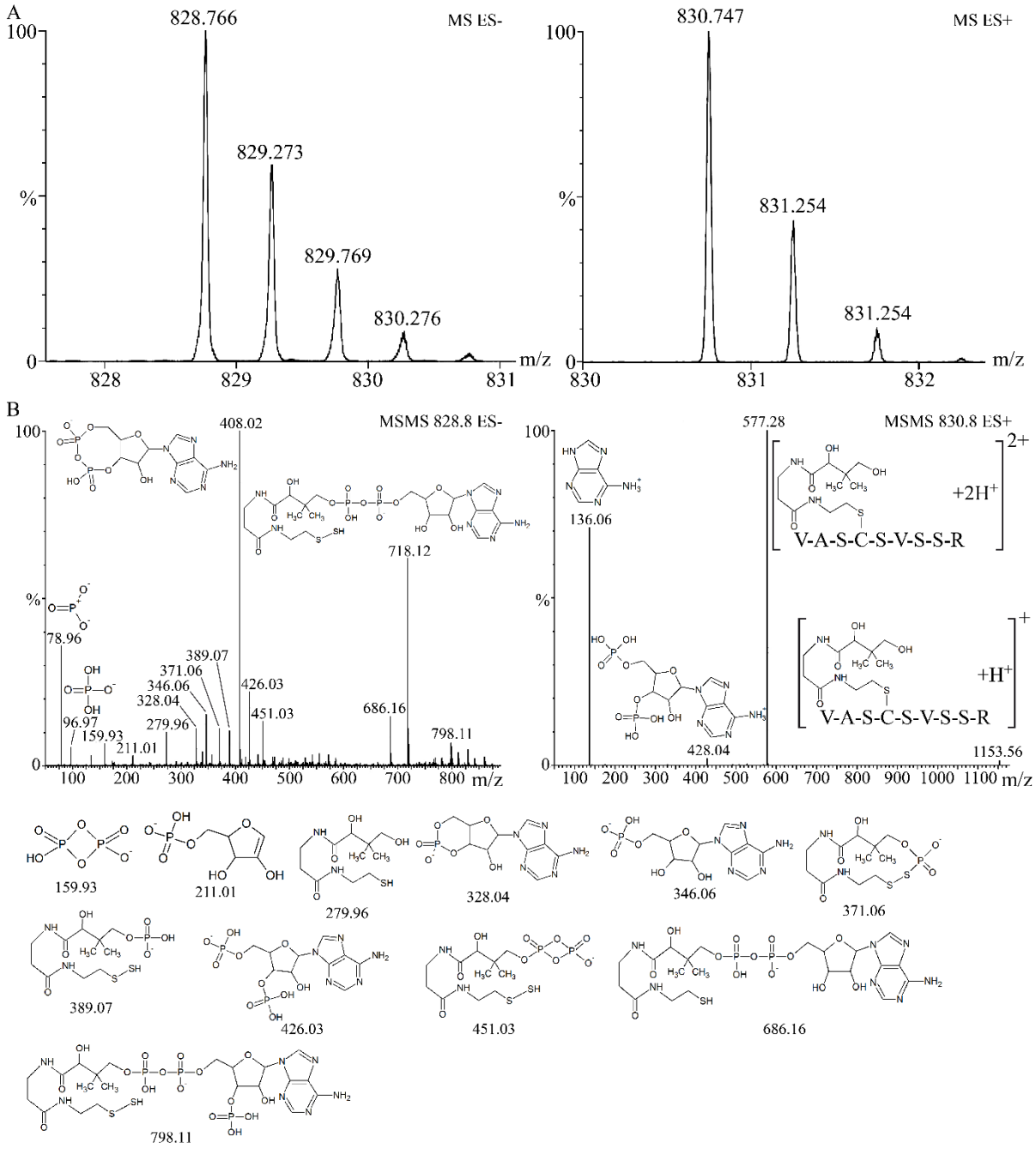

Fig. S9. MS and MS/MS analysis of the CoA-containing tryptic peptide in LarE. (**A**) LC-ESI-MS in negative (left) and positive (right) ionization modes of a doubly-charged species from the trypsin digestion of LarE that was purified in the presence of CoA. The mass of the modified peptide (1659.51 Da) corresponds to the mass of the peptide VASCSVSSR (894.41 Da) plus the mass of CoA (767.12 Da) minus the mass of two hydrogens (2.02 Da). (**B**) LC-

ESI-MS/MS fragmentation of the modified peptide in negative (left) and positive (right) ionization modes. The structures of possible fragments are shown next to the corresponding peaks or below the spectra. The ordinate represents the abundance relative to the highest peak in %.

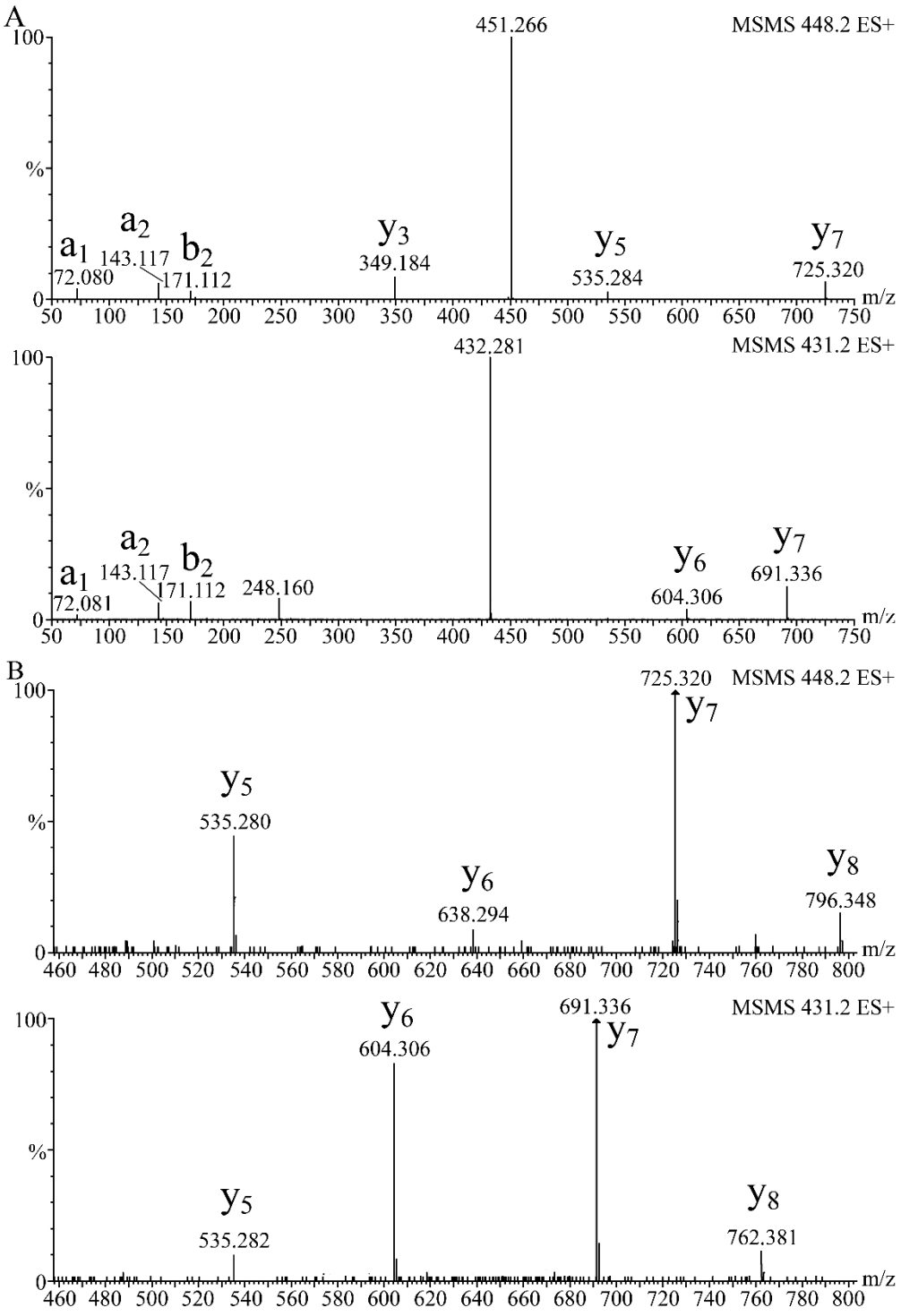
A
451.266
MSMS 448.2 ES+
100
%
0
a2
a1
143.117
b2
72.080
171.112
y3
349.184
y5
535.284
y7
725.320
m/z
50 100 150 200 250 300 350 400 450 500 550 600 650 700 750
432.281
MSMS 431.2 ES+
a2
a1
143.117
b2
72.081
171.112
248.160
y6
604.306
y7
691.336
B
725.320
MSMS 448.2 ES+
y7
y5
535.280
y6
638.294
y8
796.348
460 480 500 520 540 560 580 600 620 640 660 680 700 720 740 760 780 800
691.336
MSMS 431.2 ES+
y6
604.306
y7
y5
535.282
y8
762.381

C

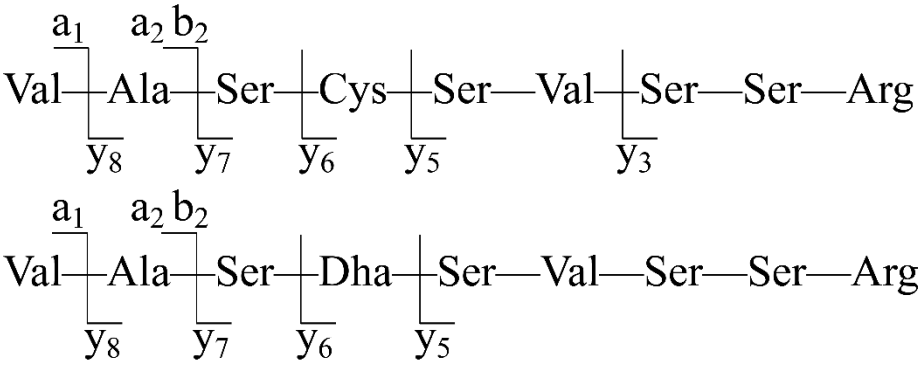
a1 a2 b2
Val—Ala—Ser—Cys—Ser—Val—Ser—Ser—Arg
y8 y7 y6 y5 y3
a1 a2 b2
Val—Ala—Ser—Dha—Ser—Val—Ser—Ser—Arg
y8 y7 y6 y5

Fig. S10. Fragmentation of the LarE tryptic peptide composed of residues 173-181 prior to and after the LarE reaction. The *m/z* 50-750 (**A**) and *m/z* 460-800 (**B**) ranges of the LC-ESI-MS/MS fragmentations are shown in positive ionization mode for the doubly-charged *m/z* 448.2 peak from trypsin digested LarE (top) and the *m/z* 431.2 peak from trypsin digested LarE 30 min after addition of the *in vitro* LarB reaction solution (bottom). The y axis is the relative abundance in %. (**C**) Schematic representations of the fragmented peptides.

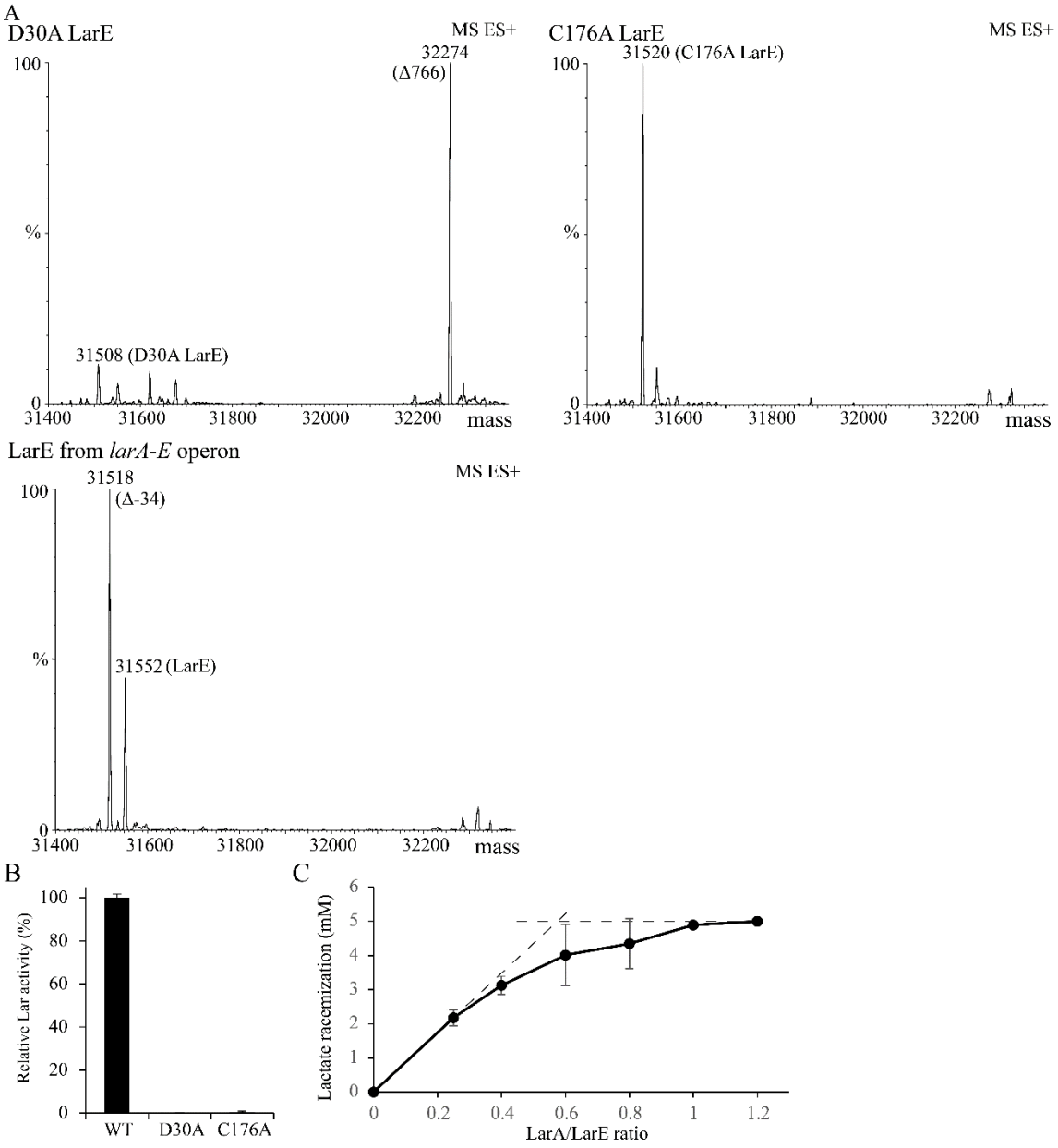

Fig. S11. LC-ESI-MS and activity of LarE. (**A**) Masses of D30A LarE (top left), C176A LarE (top right), and LarE purified from cells expressing the *larA-E* operon (bottom) purified with CoA observed in positive ionization mode. The ordinate represents the abundance relative to the highest peak in %. The numbers in parentheses indicate the mass difference from LarE (StrepII-tagged and minus the *N*-terminal methionine). (**B**) Relative Lar activity after *in vitro* activation of LarA by D30A LarE and C176A LarE variants. 100% Lar activity is that obtained for wild-type LarE. Error bars represent the SD (N=3). (**C**) Lar activity generated upon addition of LarA apoprotein (from 0 to 6 µM) to solutions incubated for 1 h

with LarE (5 µM), LarC (5 µM), $MgCl_2$ (20 mM), LarB (1 µM), NaAD (0.5 mM), $NaHCO_3$ (10 mM), $NiCl_2$ (0.1 mM) ATP (5 mM), CoA (1 mM) and cell lysate (20% volume) in Tris-HCl buffer (100 mM, pH 8). Error bars represent the SD (N=4). The dashed lines represent limiting amounts of LarA (LarA/LarE ratio ≤ 0.25) and the line of maximal Lar activity (LarA/LarE ratio ≥ 1), their intersection represents the optimal LarA/LarE ratio of 0.6±0.1 (or 1.7 LarE per LarA cofactor).

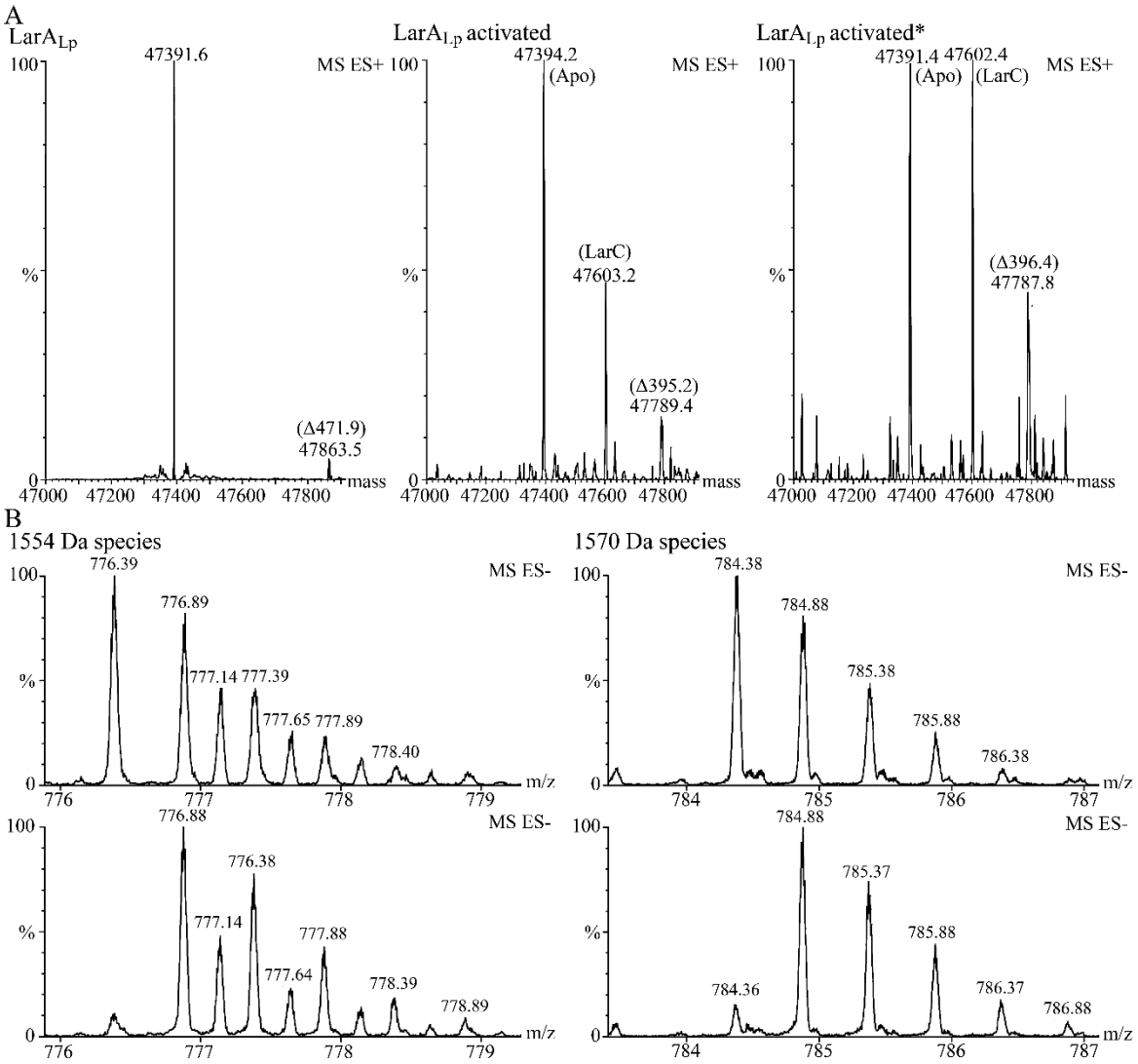

Fig. S12. LC-ESI-MS analysis of *in vitro* activated LarA. (**A**) $LarA_{Lp}$ masses as observed by LC-ESI-MS in positive ionization mode after purification ($LarA_{Lp}$) and after 90 min of *in vitro* activation with 10 µM sulfite and *in vitro*-generated P2TMN ($LarA_{Lp}$ activated) and *in vitro*-generated P2TMN* ($LarA_{Lp}$ activated*). The numbers in parentheses indicate the mass differences from the mass of the LarA apoprotein minus the *N*-terminal methionine (Apo). (**B**) LC-ESI-MS in negative ionization mode of two versions of a modified peptide from the trypsin digestion of $LarA_{Lp}$ that was activated with *in vitro*-generated P2TMN (top) and *in vitro*-generated P2TMN* (bottom). The 1554 Da and 1570 Da species are degradation products of the Lar cofactor (1). The y axis is the abundance relative to the highest peak in %.

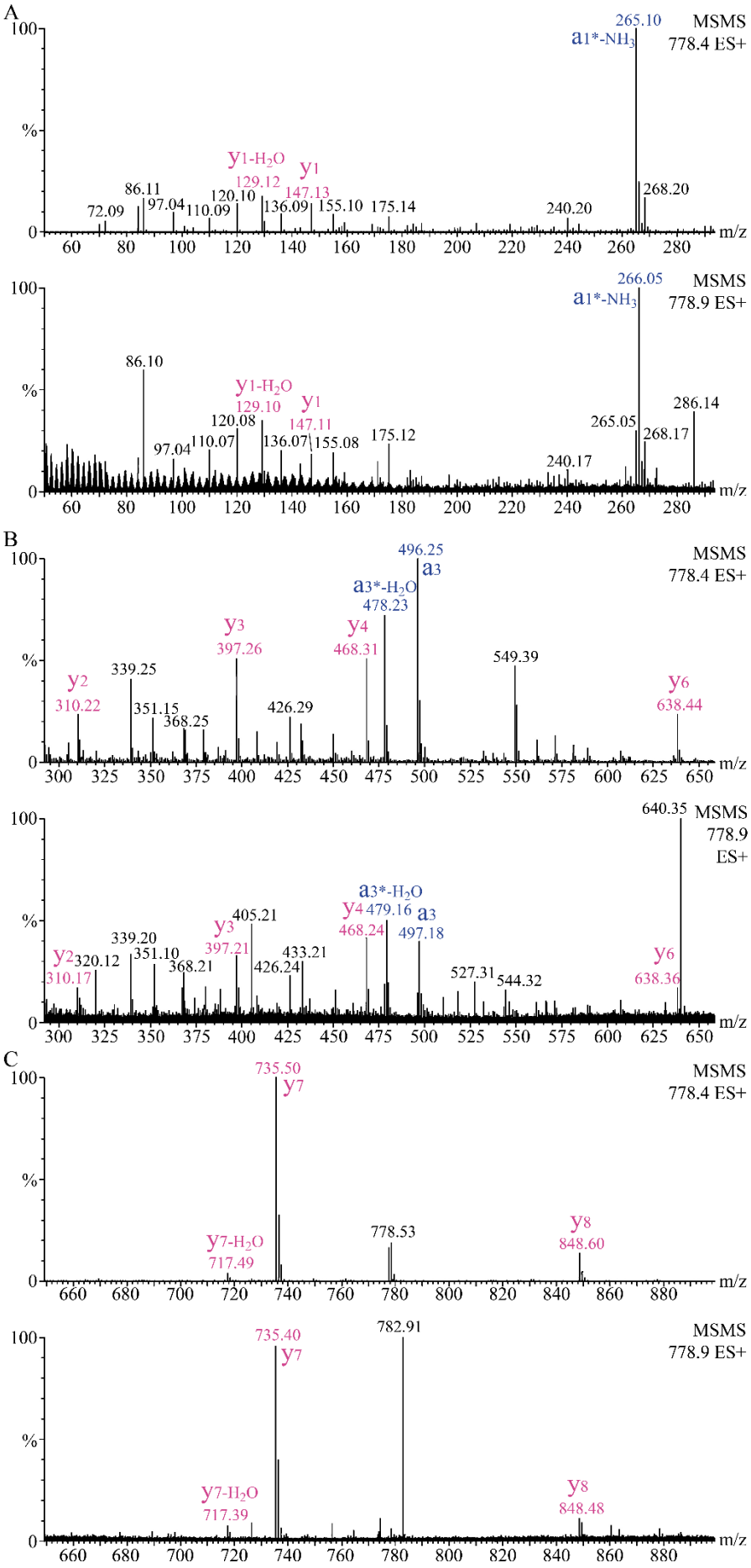
A
265.10
a1*-NH3
MSMS
778.4 ES+
y1-H2O
129.12
y1
147.13
86.11
97.04
72.09
110.09
120.10
136.09
155.10
175.14
240.20
268.20
m/z
266.05
a1*-NH3
MSMS
778.9 ES+
86.10
y1-H2O
129.10
y1
147.11
120.08
97.04
110.07
136.07
155.08
175.12
240.17
265.05
268.17
286.14
m/z
B
496.25
a3
a3*-H2O
478.23
y3
397.26
y4
468.31
549.39
y2
310.22
339.25
351.15
368.25
426.29
y6
638.44
MSMS
778.4 ES+
m/z
640.35
MSMS
778.9
ES+
a3*-H2O
y4 479.16
a3
468.24
497.18
405.21
y3
397.21
339.20
351.10
368.21
433.21
426.24
y2
320.12
310.17
527.31
544.32
y6
638.36
m/z
C
735.50
y7
MSMS
778.4 ES+
y7-H2O
717.49
778.53
y8
848.60
m/z
735.40
y7
782.91
MSMS
778.9 ES+
y7-H2O
717.39
y8
848.48
m/z

Fig. S13. LC-ESI-MS/MS analysis of a tryptic peptide generated from *in vitro* activated LarA. The ranges from *m/z* 50-290 (**A**), *m/z* 300-650 (**B**), and *m/z* 655-900 (**C**) of the LC-ESI-MS/MS fragmentation in positive ionization mode are shown for the doubly-charged 1554 Da tryptic peptide species of $LarA_{Lp}$ that was activated with *in vitro*-generated P2TMN (top) and *in vitro*-generated P2TMN* (bottom). The numbers in violet indicate the peaks corresponding to y fragments of the peptide K^{184}SVLPGIASYK. The numbers in blue indicate the peaks corresponding to the a and b fragments of the modified peptide minus ribose phosphate. The y axis is the abundance relative to the highest peak in %.

Table S1. Strains, plasmids, and primers.

Strain, plasmid, or primer	Characteristic(s) or sequence		Source or reference
Strain			
Lc. lactis			
NZ3900	MG1363 derivative		(1)
E. coli			
DH10B	F$^-$ *endA*1 *recA*1 *galE*15 *galK*16 *nupG rpsL* Δ*lacX*74 Φ80*lacZ*ΔM15 *araD*139 Δ(*ara*,*leu*)7697 *mcrA* Δ(*mrr-hsdRMS-mcrBC*) λ$^-$		Invitrogen
Plasmid			
pNZ8048	Cm^r, P_{nisA}		(2)
pGIR012	Cm^r; pNZ8048 with a 1.31-kb insert after P_{nisA} containing $larA_{Lp}$ translationally fused to DNA encoding the StrepII-tag	$LarA_{Lp}$ purification	(3)
pGIR082	Cm^r; pNZ8048 with a 1.31-kb insert after P_{nisA} containing $larA_{Tt}$ translationally fused to DNA encoding the StrepII-tag	$LarA_{Tt}$ purification	(3)
pGIR022	Cm^r; pNZ8048 with a 0.77-kb insert after P_{nisA} containing *larB* translationally fused to DNA encoding the StrepII-tag	LarB expression	(3)
pGIR026	Em^r Ap^r; pGIZ660[3] with DNA encoding the StrepII-tag translationally fused at the 3′-end of the *larB* ORF	LarB purification	This study
pGIR051	Cm^r; pNZ8048 with a 1.30-kb insert after P_{nisA} containing DNA encoding the StrepII-tag translationally fused to *larC* with an 1 bp insertion between *larC1* and *larC2*	LarC purification	(3)
pGIR072	Cm^r; pNZ8048 with a 0.89-kb insert after P_{nisA} containing *larE* translationally fused to DNA encoding the StrepII-tag	LarE purification	(3)
pGIR172	Cm^r; pNZ8048 with a 4.92-kb insert after P_{nisA} containing *larA-larE* with DNA encoding the Strep-tag translationally fused at the *C*-terminus of LarE.	LarE purification	(3)
pGIR072M1	Cm^r; pGIR072 encoding the *larE* D30A variant	LarE D30A purification	This study
pGIR072M2	Cm^r; pGIR072 encoding the *larE* C176A variant	LarE C176A purification	This study
Primers			
BT_A	3’-GGCGCTAGCTGGAGTCATCCACAATTTGAAAAGTAAGATTCAGTTAACTGAACAAGGAGAAG-5’	Construction of pGIR026	(3)
BT_B	3’-CCTGCTAGCCATTTGATTGACCATACTAGCTGAGTAGG-5’		(3)
MutE1_A	3’-TGGTGGGATCGCTAGTACCTTAGTTTTGAAGATGG-5’	Construction of pGIR072M1	This study
MutE1_B	3’- TAAGGTACTAGCGATCCCACCAGAAAAGGCCAC-5’		This study
MutE2_A	3’- GGCGTCAGCCTCTGTATCTTCACGGTTCCC-5’	Construction of pGIR072M2	This study
MutE2_B	3’- GATACAGAGGCTGACGCCACTTTATTCCAGTTC-5’		This study

1. de Ruyter PG, Kuipers OP, & de Vos WM (1996) Controlled gene expression systems for *Lactococcus lactis* with the food-grade inducer nisin. *Appl. Environ. Microbiol*. 62(10):3662-3667.

2. Kuipers OP, de Ruyter PGGA, Kleerebezem M, & de Vos WM (1998) Quorum sensing-controlled gene expression in lactic acid bacteria. *J. Biotechnol*. 64(1):15-21.

3. Desguin B, et al. (2014) Lactate racemase is a nickel-dependent enzyme activated by a widespread maturation system. *Nat. Commun*. 5:3615.